國 立 交 通 大 學

分子醫學與生物工程研究所

碩 士 論 文

釀酒酵母與畢赤酵母重組木酮糖激酶的活性分析

Activity analysis of the recombinant xylulokinase from *Saccharomyces cerevisiae* and *Pichia stipitis*

研究生：李佩君（Pei-Jiun Li）

學號：9729511

指導教授：彭慧玲 博士（Hwei-Ling Peng, Ph.D）

中華民國九十九年六月

中文摘要

石油能源危機日益嚴重，積極發展再生能源尤為當務之急，其中生質酒精之開發是相當重要的一環。酒精生產原料以纖維素、半纖維素、等植物纖維為主，纖維素與半纖維素經過生物、物理或化學處理後，分別降解成以葡萄糖為主的六碳糖與木糖(xylose)為主的五碳糖，而參與木糖發酵途徑的主要酵素包括木糖醇脫氫酶（xylitol dehydrogenase），木糖還原酶（xylose reductase）和木酮糖激酶（xylulokinase)。本研究自釀酒酵母(*Saccharomyces cerevisiae*)和畢赤酵母(*Pichia stipitis*)以聚合酶連鎖反應分別增幅選殖木酮糖激酶基因，在大腸桿菌中大量表現並進一步純化此重組的木酮糖激酶，期以活性比較分析作為改殖的依據，最終使木酮糖激酶活性在酒精生產發酵過程中不因溫度升高或過酸環境而失活。

首先，我們根據生物資訊工具分析釀酒酵母木酮糖激酶(*Sc*-XK)胺基酸的亂度變化，再以定點突變法將第88個胺基酸由絲氨酸(serine)轉變為纈氨酸（valine）。然而，*Sc*-XK和*Sc*-XK(S88V)在非原宿主中表現不具活性，我們推測此重組蛋白可能需要經過後修飾作用或修正活性測試的方法。另一方面，在畢赤酵母的木酮糖激酶(*Ps*-XK)選殖基因過程，我們意外得到一突變株在胺基酸序列中第55的位置由丙胺酸(alanine)突變為蘇胺酸(threonine)。進一步比較*Ps*-XK和*Ps*-XK (A55T)重組蛋白代謝木酮糖的活性顯示*Ps*-XK (A55T)於25℃、pH 7.8的活性比*Ps*-XK提高三倍，有趣的是，此單一氨基酸的改變不僅使*Ps*-XK最佳活性的溫度升為42℃也影響了其最適反應之pH值。

Abstract

The development of biomass ethanol as a renewable energy is currently a very important issue. The starting materials in the alcohol production process include cellulose and hemicelluloses from plant fibers. After the conversion via biodegradation, chemical or physical treatments, cellulose could be converted to six carbon sugars, mainly glucose, and hemicelluloses transformed to five-carbon sugars, mainly xylose. Xylitol dehydrogenase (XDH), xylose reductase (XR) and xylulokinase (XK) are three major enzymes involved in xylose fermentation pathway. In the study, we intend to clone the XK encoding gene using PCR from *Saccharomyces cerevisiae* and *Pichia stipitis*, and heterologously express the genes in *Escherichia coli*, and purify the recombinant proteins. After the activities comparatively analyzed, a recombinant XK that can tolerate high temperatures and acidic environments will be generated accordingly for practical use in the fermentation process.

Based on the entropy analysis (http://sdse.life.nctu.edu.tw/index.cgi) of *S. cerevisiae* XK (*Sc*-XK), site-directed mutagenesis was firstly employed to generate a change from Ser to Val (S88V). However, *Sc*-XK and *Sc*-XK (S88V) expressed in *E. coli* appeared no enzymatic activity. If a post-transcriptional modification is required for *Sc*-XK activity remains to be investigated.

On the other hand, a mutant with an amino acid change from Ala to Thr was obtained during the PCR-cloning of XK from *P. stipitis* (*Ps*-XK) and named *Ps*-XK (A55T). Interestingly, activity analysis revealed *Ps*-XK (A55T) had a 3-fold higher specific activity than *Ps*-XK at 25℃, pH 7.8. Moreover, single amino acid change of XK affected not only its suitable temperature, which increased to 42℃, but also caused the pH shift.

致謝

還記得兩年前我還是一個懵懵懂懂，剛畢業的大學生，轉眼間研究所的生涯即將結束。當初要從熟悉的台北搬到陌生的新竹，心裡是既期待又怕受傷害。在新竹的這兩年，我學到了很多，除了實驗上的進步，表達能力，更磨練自己對事情處理的態度和方法。

這兩年的生活，我最感謝的人是我的指導教授彭慧玲老師，由於老師耐心認真的教導也常常鼓勵我，讓我能很快地建立自己的實力和信心。每一周要跟老師面對面談實驗之前都會很緊張和徬徨，但每次和老師討論完總是會豁然開朗，讓我獲益良多，真的覺得自己很幸運可以遇到老師，對彭老師有說不完的感謝。

還要感謝清華大學張晃猷老師擔任我的口試委員以及張老師實驗的夥伴，能抽空參與我的口試預講，給予實驗上的建議及協助，以及交通大學楊裕雄老師能擔任我的口試委員，在口試中給予我實驗上不同的觀點以和指導，以及非常用心的修正我的碩士論文。

感謝動感的丸子學姊在實驗上的指導與幫助，隨和的個性也製造了很多歡樂；身材很好的靜柔學姊總是在我遇到困難時，拉我一把，開導我並幫助我解決問題，常常因為她的一句話，讓我覺得事情其實沒有那麼複雜；感謝幽默風趣的健誠學長和新耀學長在我初進實驗時，細心耐心地教導我；溫柔的惠如學姊能抽空帶我做實驗；楊裕雄老師

實驗室的秀華學姊在實驗上幫助我許多；感謝我的好同學們，有點悶騷的其駿、嘴壞人不壞的哲充和適合當女強人的家華這兩年來的幫助與支持，從他們身上我學到了很多；實驗室活潑又可愛的學妹崴云和品瑄及學弟豪君為實驗室增添很多歡樂；感謝認識多年個性海派人很好的大學同學毓娟，總是跟我一起發牢騷，要感謝的人實在太多，總之超級感謝這些和我一起創造回憶的同伴，我會永遠記得。

最後要最感謝我的家人，我的父母、哥哥、姊姊和育騏的家人，他們總是在我身邊，默默的付出，分享我的喜怒哀樂，他們的支持是我努力完成學業的最大動力，真的很開心身邊有這麼多人照顧我，對他們的感謝不是三言兩語就可以說完，真的很謝謝你們，我愛你們唷！

從零開始的我，在這兩年間，因為身邊許多人的支持與幫助，讓我成長了許多，即將邁入人生的另一個旅程，我要繼續努力，希望大家都能順順利利，心想事成。

佩君

民國99年7月21日 筆於新竹交通大學竹銘館分子調控實驗室

Contents

Table contents

Page

Figure contents

Page

Abbreviation

ATP	adenosine triphosphate
bp	base pair (s)
DNA	deoxyribonucleic acid
EDTA	ethylenediamine-tetraacetic acid
IPTG	isopropyl-1-thio-β-D-galactopyranoside
Kb	kilobase (s)
kDa	kiloDalton (s)
LB	Luria-Bertani
LDH	lactose dehydrogenase
mM	millimolar
NAD	nicotinamide adenine dinucleotide
NADH	nicotinamide adenine dinucleotide (reduced form)
nm	nanometer
ORF	open reading frame
PAGE	polyacrylamide gel electrophoresis
PCR	polymerase chain reaction
PEP	phosphoenolpyruvate
PK	pyruvate kinase

PPP	pentose phosphate pathway
rpm	revolutions per minute
SDS	sodium dodecyl sulfate
XDH	xylitol dehydrogenase
XK	xylulokinase
XR	xylose reductase
μM	micromolar

Introduction

Energy crisis and biofuel development

The recent energy shortage and environmental crisis have demanded facile, low-cost, environmentally friendly, and nontoxic routes for producing novel functional materials that can be commercialized in the near future (Hu et al., 2010). The need for renewable energy as well as the request to reduce green house effect is particularly urgent. In response, the development of biomass ethanol is currently a very important issue and the use of bioconverted fuels offers solutions to many environmental problems (Katahira et al., 2004).

Bioethanol has been produced mainly from sugar-containing or starchy biomass such as sugarcane and corn as the raw materials. As sugar-containing or starchy biomass is largely used for food and animal feed, the competition for its use as food or fuel is hence aroused .As a result, lignocellulosic production for bioethanol becomes an eager research worldwide. Lignocellulosic biomass, such as agricultural and forestry residues, waste paper, and industrial wastes, has been recognized as an ideally inexpensive carbohydrates source o for fermentation into fuel ethanol (Katahira et al., 2004, Matsushika et al., 2009a).

The main structural components of lignocellulosic biomass are cellulose, hemicellulose, and lignin. Of these, only cellulose and hemicellulose can be used as raw materials to produce ethanol by chemical or enzymatic hydrolysis (namely saccharification) (Matsushika et al., 2009a). Pretreated cellulose can be enzymatically hydrolyzed either prior to fermentation or by adding the cellulase and inoculum together for

simultaneous saccharification and fermentation, (SSF). SSF which gives higher ethanol yields requires lower amounts of enzyme because end product inhibition from cellobiose and glucose formed during enzymatic hydrolysis. Nevertheless, the enzyme added and culture condition for SSF has to be compatible with respect to pH and temperature (Dien et al., 2003).

Through biological, physical or chemical treatment produces of cellulose, mainly six carbon (6C) sugars are produced. On the other hand, xylose is the most abundant pentose sugar(up to 40%) in hemicellulosic hydrolysates (Chandrakant P, 1998). Metabolism of xylose has been investigated extensively for the manufacture of fuel ethanol(Lynd et al., 1991). It is recognized nowadays that how to efficiently ferment xylose to ethanol to is crucial for the production of this renewable liquid fuel (Dmytruk et al., 2008).

The current status for fuel ethanol production

Remarkable successes have been reported in the engineering of Gram-negative bacteria including *Escherichia coli*, *Klebsiella oxytoca*, and *Zymomonas mobilis*. These bacteria are naturally able to use a wide spectrum of sugars, and hence a lot of work has concentrated on engineering them for the selective production of ethanol (Dien et al., 2003).

The construction of *E. coli* strains to selectively produce ethanol has been one of the first successful applications of metabolic engineering (Ingram et al., 1987). *E. coli* has several advantages as a biocatalyst for

ethanol production, including the ability to ferment a wide spectrum of sugars, no requirements for complex growth factors, and prior industrial use. The major disadvantages are a narrow pH growth range (ca. pH 6.0 –8.0), less hardy cultures compared to yeast, and public perceptions of the danger potential of *E. coli* strains (Dien et al., 2003). In *E. coli*, the interconversion of xylose and xylulose is catalyzed by the *xylA* gene encoding xylose isomerase. Overproduction of xylose isomerase resulted in mainly insoluble proteins in *S. cerevisiae* and catalytically inactive (Sarthy et al., 1987, Matsushika et al., 2009a).

Z. mobilis is an unusual Gram-negative microorganism which has not only a homoethanol fermentation pathway but also a high tolerance to ethanol. Moreover, it has much higher specific ethanol productivity than *S. cerevisiae* (Skotnicki et al., 1982). Therefore, *Z. mobilis* has been used in the 1970s and 1980s for conversion of starch to ethanol and industrial scaled trials have been carried out successfully (Doelle MB, 1989, Millichip RJ, 1989). However, *Z. mobilis* ferments only glucose, fructose and sucrose and hence not well suited for the biomass conversion (Dien et al., 2003). Instead, *S. cerevisiae* is still preferred by the industry because of its hardiness.

However, many attempts to express heterologous xylose isomerase (*xylA*) genes in *S. cerevisiae* have failed (Sarthy et al., 1987, Amore R, 1989, Moes CJ, 1996, Gárdonyi M, 2003). Overexpression of the *xylA* from the fungi *Piromyces* or *Orpinomyces*, or the bacteria *Thermus thermophilus* in *S. cerevisiae* have been the only successful instances for the anaerobic production of ethanol from xylose (Walfridsson M, 1996,

Kuyper M, 2003, Kuyper M, 2004, Kuyper M, 2005a, Madhavan A, 2008).

Fermentation of Glucose

D-Glucose is a common substrate in the food industry and is cheap and readily available compared to D-xylose. It is hence whether xylitol could be produced from D-glucose has been an attractive issue. However, few natural microorganisms that produce xylitol from D-glucose are known. The species *Bacillus*, *Zygosaccharomyces*, *Aureobasidium*, *Torula*, and *Candida* can convert D-glucose to other sugars and sugar alcohols such as D-ribose, D-arabitol, and erythritol (Toivari et al., 2007).

A recent metabolic model that combines induction of sugar transporters with the kinetic characteristics of the various proteins predicts that xylose transport by *S. cerevisiae* is maximal when the glucose concentration is near zero since the presence of glucose represses the high affinity hexose transporters that are responsible for xylose assimilation (Bertilsson et al., 2008, Katahira S, 2008).

When the glucose transporter of *P .stipitis* Sut1 was expressed in a xylose-utilizing *S. cerevisiae*, it enhanced xylose fermentation to ethanol (Van Vleet and Jeffries, 2009, Katahira S, 2008).

Xylose fermentation pathway

Several approaches which including modeling, expression analysis, and flux analysis followed by the targeted deletion or altered expression of key genes have been employed to engineer xylose metabolism (Jeffries,

2006).

Potential host for xylose fermentation requires an efficient pentose phosphate pathway (PPP) linked with xylose-to-xylulose pathway to glycolysis (Matsushika et al., 2009c) : Xylose is converted to xylulose by two oxidoreductases involving cofactors NAD-(P)-H and NAD-(P) $^{+}$. First, xylose is reduced to xylitol by NAD-(P)-H-dependent xylose reductase (XR; EC1.1.1.21) (Bruinenberg PM, 1984, Verduyn et al., 1985, Bolen PL, 1986, Rizzi M, 1988). Xylitol is then oxidized to xylulose by NAD^{+}-dependent xylitol dehydrogenase (XDH; EC 1.1.1.9)(Bolen PL, 1986);(Rizzi M, 1988, Rizzi M, 1989, Wang VW, 1990); The xylulose is phosphorylated into xylulose 5-phosphate (X5P) via xylulokinase (XK; EC 2.7.1.17) (Deng XX, 1990); (Rodriguez-Pena JM, 1998). Finally, X5P is further metabolized via the pentose phosphate pathway (PPP) and glycolysis. As this reaction utilizes adenosine triphosphate (ATP), the reaction rate is dependent on the energy charge and the phosphorylation potential of the cell (Matsushika et al., 2009a)(Fig.1).

Studies on XR and XDH

Natural xylose-fermenting *P .stipitis* excretes substantial amounts of the by-product xylitol. The excretion of xylitol has been mainly ascribed to the difference in coenzyme specificities between the mainly NADPH-dependent XR and strictly NAD $^{+}$-dependent XDH. Thus, during the XR and XDH reactions, excess NADH accumulates leaving a shortage of NAD $^{+}$, resulting in an intracellular redox imbalance (Bruinenberg PM, 1983, Kötter P, 1993). In *P .stipitis,XYL1* and *XYL2*

genes encode XR and XDH respectively (Chu and Lee, 2007). *P. stipitis* is one of the few yeast species that possess both NADPH- and NADH-specific XR (*Ps*-XR),despite the preference for NADPH providing the yeast with the ability to excrete less xylitol during xylose fermentation (Verduyn et al., 1985). *Pachysolen tannophilus* also possesses dual specific XR, produces more xylitol than *P. stipitis* (Debus D, 1983).

Several metabolic engineering strategies have attempted to improve xylose fermentation using *Ps*-XR and *Ps*-XDH expressing *S. cerevisiae* strains. Recent studies have also showed that high activity of both *Ps*-XR and *Ps*-XDH is important for generating an efficient xylose-fermenting recombinant *S. cerevisiae* strain (Jeppsson et al., 2003, Karhumaa et al., 2007, Matsushika and Sawayama, 2008).

However, substantial amount of the xylitol produced in the recombinant *S. cerevisiae* strains expressing *Ps*-XR and *Ps*-XDH reduces the ethanol yield (Kötter P, 1993, Tantirungkij M, 1993). I n order to increase the ethanol yield, higher level of XDH relative to XR has been experimentally designed (Walfridsson M, 1997, Eliasson A, 2001, Jin YS, 2003, Karhumaa et al., 2007).

Ethanol production from xylose in yeast

The characteristics required for an industrially suitable microorganism include capability to ferment pentose and hexose, ethanol productivity, ethanol tolerance, robust grower and simple growth requirements. In addition, the microorganisms are able to grow in undiluted hydrolysates,

acidic pH or higher temperatures(Dien et al., 2003).

S. cerevisiae, which is a very safe microorganism, plays a major role in industrial bioethanol production. The yeast has several advantages due to its successful exploitation in the fermentation industry, high level tolerance to ethanol, highly developed knowledge of its genetics and physiology, high ethanol productivity, and tolerance to compounds present in the hydrolysate (Matsushika et al., 2009a, Eliasson et al., 2000, Ni et al., 2007).

In an industrial alcoholic fermentation, accumulation of lactic acid and acetic acid are always found. A volume of research has been conducted on the inhibitory effects of lactic acid and acetic acid on yeast growth and metabolism. The interaction of lactic acid and acetic acid on ethanol production by *S. cerevisiae* in corn mash, as influenced by temperature has also been examined(Graves et al., 2007).

The research associated with temperature mainly concerned the thermotolerant methylotrophic yeast *Hansenula polymorpha* which is capable of alcoholic fermentation of xylose at elevated temperatures (45 – 48°C). Such property defines this yeast as a good candidate for the development of an efficient process with simultaneous saccharification and fermentation (Dmytruk et al., 2008).

Among the native xylose-fermenting yeasts, *Candida shehatae, P. tannophilus,* and *P. stipitis* can ferment xylose to ethanol with high yields (Jin et al., 2002). However, relative to the glucose fermentation by *S. cerevisiae,* these xylose-fermenting yeasts display lower ethanol production rates (Jin et al., 2002).

S. cerevisiae is highly effective for the production of ethanol from hexose sugars but incapable of fermenting xylose (Matsushika and Sawayama, 2008). Nevertheless, *S. cerevisiae* can slowly metabolize xylulose via xylulokinase (XK) to produce ethanol (Wang, 1980, Lee et al., 2003).

Xylose is the dominant pentose sugar in hydrolysates of lignocellulosic biomass. Therefore, a number of strategies have been applied to engineer yeasts with capability of efficiently producing ethanol from xylose. These include increasing xylose transport, changing the intracellular redox balance, and overexpression of XK and pentose phosphate pathway (Matsushika et al., 2009a).

In general, the engineering *S. cerevisiae* for xylose utilization has focused on adapting the xylose metabolic pathway from *P. stipitis* such as cloning the XR and XDH encoding genes from *P. stipitis* and heterologously expression of the genes in *S. cerevisiae* (Jin et al., 2002, Yong-Su Jin, 2003). However, the *S. cerevisiae* XK appeared to be active also on D-ribulose and hence *P. stipitis* XK which is specific on D-xylose is better used for the propose of engineering xylulose metabolism (Jin et al., 2002).

Early studies of xylose fermentation in *S. cerevisiae* revealed that the overexpression of *XKS1* is essential for growth and fermentation. In contrast, Rodriguez-Pena *et al.* reported that the overexpression of *XKS1* in *S. cerevisiae* inhibits the growth on D-xylulose (Rodriguez-Pena et al., 1998). Other researchers have found that overexpression of the *S. cerevisiae XKS1* along with *PsXYL1* and *PsXYL2* increased ethanol

production but decreased xylitol production from xylose (Ho et al., 1998, Ni et al., 2007). Similarly, overexpression of *PsXYL3* along with high levels of *PsXYL1* and *PsXYL2* in *S. cerevisiae* was found to entirely inhibit cell growth on xylose, whereas *S. cerevisiae* transformant expressing *PsXYL3* at a moderate level was able to grow on xylose (Yong-Su Jin, 2003).

Other studies by Johansson *et al.* noted that overexpression of *S. cerevisiae XKS1* reduced xylose consumption by 50 to 80%, even though it increased the yield of ethanol (Johansson et al., 2001). Overexpression of *S. cerevisiae XKS1* could be inhibitory for several reasons: First, *S. cerevisiae* might not possess a guard system to prevent excessive ATP consumption and the rapid ATP depletion would then inhibit the cell growth. Second, the PPP capability in *S. cerevisiae* might not be enough to control metabolic flux at a steady state for ATP synthesis since excess XK activity could result in accumulation of X5P and depletion of ATP. Third, it is possible that X5P itself is toxic to the cells (Yong-Su Jin, 2003).

The relationship between structural entropy and thermal stability

Protein thermal stabilization has been the focus of many experimental and theoretical research works, but the molecular basis of thermal stability appears to be of diverse origin. Structural analysis has revealed various structural features that characterize the thermal stability of proteins.

Thermophilic proteins tend to have stronger electrostatic interactions

(more surface charged residues, surface salt bridges, hydrogen bonds), more disulfide bridges, higher degrees of hydrophobic packing in the core regions, more pronounced bias in amino acid content on the exposed regions, shorter loop structures, higher conformational rigidity and more secondary structural elements such as α-helices and β-sheets.

However, despite these many structural features, they validated the linear relationship by compiling a large dataset comprised of 1153 sequences and found that most protein families still display similar linear relationships. They also observed a good linear relationship between the average structural entropy and the melting temperatures for adenylate kinase and its chimeric constructs.

The research suggested that the multitude of interactions involved in thermal stabilization may be generalized into the tendency of proteins to maintain local structural conservation. The linear relationship between structural entropy and protein thermostability should be useful in the study of protein thermal stabilization.

Objective of the study

In this study, we aim to obtain large amounts of a highly efficient and specific XK protein which could be added to the fermenting yeast at a certain stage without impairing the cell growth. The XK encoding genes from *P. stipitis* and *S. cerevisiae* will be isolated by PCR amplification. The genes will then be cloned into an expression vector and heterologously expressed in *E .coli*. Finally, the overexpressed protein will be purified and the enzyme properties characterized and compared.

Site-directed mutagenesis will also be employed for generating an efficient and specific XK activity.

Materials and methods

Yeast and bacteria strains, plasmids, and growth conditions

Bacterial strains and plasmids used or constructed in this study are listed in Table 1 and Table 2 respectively. Genomic DNA for PCR amplification was prepared from *Pichia stipitis* and *Saccharomyces cerevisiae* grown in YPD (10 g/l yeast extract, 20 g/l peptone, 20 g/l dextrose) broth or on YPD agar at 30°C. All bacteria were propagated at 37°C in Luria-Bertani (LB 10 g tryptone, 5 g/l yeast extract, 10 g/l sodium chloride) broth or on LB agar supplemented with appropriate antibiotics including kanamycin (25 μg/ml) and ampicillin (100 μg/ml) when needed.

Isolation of genomic DNA from Pichia stipitis and Saccharomyces cerevisiae

The yeast was grown for 20-24 h at 30°C in YPD broth. The culture was then transferred into a microcentrifuge tube and subjected to centrifugation at 13000 rpm for 5 min. The supernatant was decanted and the cell pellet was resuspended in 200 μl lysis buffer (2% Triton X-100, 1% SDS, 100 mM NaCl, 10 mM Tris-HCl, and 1 mM EDTA, pH 8.0). The suspension was immersed on ice for 5 min, heated to 95°C~100°C for 5 min and mixed with 200 μl chloroform and by vortex for 2 min.

After centrifugation at 13000 rpm for 3 min, the upper aqueous phase was transferred into a microcentrifuge tube containing 400 μl ice-cold 100% ethanol, mixed by inversion or gentle vortex and then stored at -80°C for 1 h. Finally DNA pellet was collected after precipitation by

centrifugation at 13000 rpm for 5 min and washed with 1 ml 70% ethanol. The DNA pellet was air-dry at 37°C for 1 h, resuspended in pure H_2O at 60°C, and stored at -20°C until required.

DNA manipulation

Plasmids were purified by using the High-Speed Plasmid Mini kit (Geneaid, Taiwan). All restriction endonucleases and DNA modifying enzymes were purchased from either New England Biolab (Beverly, MA) or MBI Fermentas (Hanover, MD), and were used according to the recommendation of the supplies. PCR amplifications were performed with Taq DNA polymerase (MDBio, Inc, Taiwan). PCR products or DNA fragments were purified using the Gel/PCR DNA Fragments Extraction kit (Geneaid, Taiwan). Primers used in this study were synthesized by MDBio, Inc, Taiwan.

Preparation of competent cells for electroporation

A single colony of freshly grown *E. coli* was inoculated in a flask containing 25 ml of LB medium and cultured overnight at 37°C with vigorous aeration (200 rpm in a rotary shaker). The overnight culture was then inoculated into 500 ml prewarmed LB medium and grown with agitation aeration (200 rpm in a rotary shaker) at 37°C. The bacterial density was measured every 20 min till the OD_{600} reached 0.4 and the cultural flask moved to an ice-water bath for 20 min with occasional swirl to ensure that cooling occurs evenly.

Finally, the cultures were transferred to ice-cold centrifuge bottles and

the cells were harvested by centrifugation at 13000 rpm for 20 min at 4°C. The supernatant was decanted and the cell pellet was resuspended in 300 ml of ice-cold pure H_2O and again harvested by centrifugation at 13000 rpm for 20 min at 4°C. The cell pellet was resuspended in 150 ml of ice-cold 10% glycerol and collected by centrifugation at 13000 rpm for 20 min at 4°C. The procedure was repeated once and the pellet was resuspended in 1 ml of ice-cold GYT medium (10% glycerol, 0.125% yeast extract, and 0.25% tryptone). The cell suspension was dispensed 40 µl aliquots into sterile, ice-cold 1.5 ml microfuge tubes and stored at -80°C until required.

Software for analysis of protein structure and amino acid structural entropy

Structural predictions were performed using Swiss-Model (http://swissmodel.expasy.org//SWISS-MODEL.html) and multiple sequence alignments were performed using Vector NTI 6.0. The sequence derived structure entropy was analyzed according to the provided software at http://sdse.life.nctu.edu.tw/index.cgi.

Site-directed mutagenesis

XK mutants were produced using the QuikChange site-directed mutagenesis method (Stratagene) recommended by the manufacturer. The primers used are listed in Table 3 and the resulting plasmid was respectively termed in Table 2 and the mutant XK proteins were expressed in *E. coli* BL21 (DE3) or *E. coli* NovaBlue (DE3).

Constructions of the recombinant His_6-tagged proteins

The XK expression plasmid pET30-Sc-XK was generated by PCR-amplification of the coding sequence of XK gene from *S. cerevisiae* using primer pair PJ036 and PJ037 (Table 3), the amplified DNA was restricted by EcoRI/SalI and then ligated into the pET-30b vector. Similar approach was used to generate other recombinant plasmids such as pET30-Ps-XK. The coding region was PCR amplified using primer pair PJ038 and PJ039 (Table 3).

Overexpression and purification of the His_6-tagged proteins

Bacterial cells were incubated in 500 ml of LB medium at 37°C with shaking until OD_{600} reached 0.5. Isopropyl-1-thio-β-D-galactopyranoside (IPTG) was then added to a final concentration of 0.5 mM and the growth was continued for 16-20 h at 22°C.

Subsequently, the cells were harvested by centrifugation at 10000 rpm for 20 min at 4°C, resuspended in binding buffer (20 mM Tris-HCl, 500 mM NaCl, 5 mM imidazole, pH 7.9), the cells disrupted by sonication and then the cell debris removed by centrifugation at 13000 rpm for 10 min at 4°C.

Finally, the His_6-tagged proteins were purified from the supernatant via affinity chromatography using His-Bind resin (Novagen). The washing buffer is consisted of 20 mM Tris-HCl, 500 mM NaCl, 70 mM imidazole, pH 7.9 and the elution buffer consisted of 20 mM Tris-HCl, 500 mM NaCl, 80mM imidazole, pH 7.9.

After the protein-bound resins washed several times with the wash

buffer and the protein eluted using the elution buffer, purity of the collected fractions were analyzed by SDS-PAGE. Finally, the purified His_6-tagged kinase was dialyzed against 500 ml of the buffer containing 0.1 g KCl, 4 g NaCl and 1.5 g Tris-HCl, pH 7.8.

SDS-polyacrylamide gel electrophoresis

Before subjected to gel electrophoresis, the proteins in lysis buffer (0.0625 M Tris-HCl buffer pH 6.8, 4% SDS, 10% glycerol, 0.002% bromophenol blue, 100 mM 2-Mercaptoethanol) was heated for 15 min at 95°C. Aliquots of the protein samples were applied to a 13.5% SDS polyacrylamide slab gel and electrophoresis was carried out at room temperature until the tracking dye ran off the bottom of the slab gel. The gel was then stained for 30 min with Coomassie blue (0.5 g Brilliant Blue R, 45% methanol, and 10% acetic acid) and destained briefly in destain I buffer (500 ml H_2O, 400 ml methanol and 100 ml acetic acid) for 15 min and in destain II buffer (880 ml H_2O, 50 ml methanol and 70 ml acetic acid) for 30 min.

Circular dichroism spectrum analysis

The CD spectra of wild-type and the mutant were recorded by using a CD spectrophotometer (AVIV 62A DS) with 1-mm path length cell, 0.5 nm wavelength step, and an averaging time of 3×10^{-1} s. The protein samples were adjusted to 2.5 μM before measurement. The CD spectra signals were collected from 190 nm to 260 nm at 25°C in 10 mM Tris-HCl, pH 7.4 and averaged over three scans (Lee et al., 2008).

Xylulokinase activity measurement and kinetics characterization

Activity of the purified XK was determined according to the described spectrophotometric assay (Dmytruk et al., 2008) with some modifications and the condition is summarized in Table 4. The enzymatic activity was determined by monitoring the change in absorbance at 340 nm that accompanies the oxidation of NADH to NAD^+.

The XK activity assay mixture contained 5 mM $MgCl_2$, 0.2 mM NADH, 1 mM phosphoenolpyruvate, 8.5 mM D-xylulose, 10 U lactate dehydrogenase, 1.5 U pyruvate kinase, and 2 mM ATP in 50 mM Tris-HCl, pH 7.8. The reaction at 25°C was started with addition of purified protein.

The K_M and V_{max} for xylulose and ATP were determined independently using standard assay conditions (Dmytruk et al., 2008). Constants for xylulose as substrate were measured at 42°C by holding constant ATP concentration and varying xylulose level with 0.0425 mM, 0.2125 mM, 0.425 mM, 2.5 mM or 4.5 mM. Similarly, ATP kinetic measurements at 42°C were made by holding constant xylulose and varying ATP concentration with 0.05 mM, 0.1 mM, 0.5 mM, 1 mM or 2 mM. K_M and V_{max} were calculated by fitting the data to Michaelis-Menten equation (Di Luccio et al., 2007).

Temperature effect on Xylulokinase activity

This assay was performed essentially as described above except that the reaction temperature varied at 20°C, 25°C, 37°C, 42°C, 50°C or 60°C.

Analysis of pH effect on Xylulokinase activity

This assay was performed essentially as described above except that the reaction pH varied with pH 6.5, pH 7, pH 7.5 of 50 mM Tris-HCl or pH 7.5, pH 8, pH 8.5, pH 9 of 50 mM MPOS buffer at 25°C.

Results

Genetic and sequence analysis of XK from S. cerevisiae and P. stipitis

The research exhibited that the XK of *P. stipitis* and *S. cerevisiae* belong to the FGGY and FGGY family of carbohydrate kinases which included D-xylulokinase (EC 2.7.1.17), L-xylulokinase (EC 2.7.1.53), glycerol kinase (EC 2.7.1.30), glucokinase (EC 2.7.1.12), and L-fuculokinase (EC 2.7.1.51) (Jin et al., 2002). The XK gene *XYL3* from *P. stipitis* encodes a polypeptide of 624 amino acids and *XKS1* from *S. cerevisiae* coding for a polypeptide of 600 amino acids (Fig. 2). Approximately 41.3% sequence identity was found between the two XK, which have been demonstrated to be able to metabolize xylulose (Matsushika et al., 2009b).

As shown in Fig. 3, the N-terminal LGFDLSTQQLK peptide common to sugar kinases for phosphate binding (Jin et al., 2002) appeared to be also conserved. Comparison analysis revealed *Ec*-XK and *Ps*-XK, and *Ec*-XK and *Sc*-XK shared sequence identity of 13.6% and 16.8% respectively. The two conserved aspartate residues, Asp17 and Asp27, located at the N-terminal domain I required for *Ec*-XK interaction with the ATP-associated Mg^{2+} (Di Luccio et al., 2007) were also present in *Ps*-XK and *Sc*-XK. In order to have a negative control for the following activity analysis, a single residue change from Asp17 to Ala on *Ps*-XK was generated using the site-directed mutagenesis method (Appendix 1) and the mutant named *Ps*-XKD17A.

Search for the critical residues of S. cerevisiae XK amino acid sequence on the base of entropy difference

We explored the relationship between structural entropy profile and protein thermal stability by the approach offered a straightforward way to compute the structural entropy directly from the query sequence. It may be used as a useful tool to screen mutant candidates for thermophilic sequences in a high throughput way (Chan et al., 2004).

The XK of *S. cerevisiae* and *P. stipitis* belong to the FGGY family, of which the FGGY region was selected for site-directed mutagenesis. After the conserved residues eliminated, the rest of *Sc*-XK sequences were selected for the analysis of entropy change (Fig. 4). The entropy change was calculated by replacing the target amino acid with other nineteen amino acids and the minimum entropy state was selected.

As shown in Table 5, six residue substitution including S47E, S88V, G169C, S253W, S254M, and S255W with a maximal drop of the entropy were identified. To verify if each of the residue change increases the protein thermal stability as suggested by Chan et al., (Chan et al., 2004), a Ser88 to Val88 alteration of *Sc*-XK was generated using the site-directed mutagenesis method (Appendix 1) and the mutant named *Sc*-XKS88V.

Construction, expression and purification of the recombinant XK

In addition to *Ps*-XKD17A and *Sc*-XKS88V mutants, a *Ps*-XK mutant probably resulted from random mutation during PCR cloning of *Ps*-XK was obtained and named *Ps*-XKA55T (Fig. 3).

The wild-type and mutant XK cloned into pET30b were expressed in *E.*

coli BL-21 (DE3) or *E. coli* NovaBlue (DE3) and the proteins purified by nickel affinity chromatography. Its purity was confirmed on a SDS-polyacrylamide gel and stained with Coomassie Blue. As shown in Fig. 5, expression of *Sc*-XK and *Sc*-XKS88V could barely be detected. By contrast, overexpression of *Ps*-XK (Fig. 6A) and *Ps*-XKA55T (Fig. 6B) were observed. Nevertheless, all the recombinant proteins could be purified to homogeneity (Figs. 5 and 6).

Circular dichroism analysis of the recombinant proteins

Prior to the activity measurement of the recombinant XK, the activity alteration caused by its conformational changes has to be excluded. The applications of CD spectroscopy could be categorized in various regions of biological studies such as conformational assessments of proteins and nucleic acids. Protein secondary structure can be determined by CD spectroscopy in the 'far-UV' spectral region (190–250 nm)(Ranjbar and Gill, 2009).

As shown in Fig.7, the CD spectra of *Sc*-XK and *Sc*-XKS88V are identical. Overlapping CD spectra *Ps*-XK, *Ps*-XKA55T and *Ps*-XKD17A showing a minimum point at 208 nm and 222 nm, a typical spectrum of high α-helix content protein (Ranjbar and Gill, 2009), were also observed (Fig. 8). These indicate no major alteration of the secondary structure of the mutant proteins.

Activity measurement of the XK

The XK activity was determined using the assay condition summarized

in Table 4. Surprisingly, no detectable activity could be observed for *Sc*-XK or *Sc*-XKS88V. On the other hand, *Ps*-XK and *Ps*-XKA55T both exhibited enzymatic activity (Fig. 9). As shown in Fig. 9, no activity for *Ps*-XKD17A was found further supports that the Asp residue is essential for the XK activity.

Comparative analysis of the specific activity at 25℃, pH 7.8 revealed that *Ps*-XKA55T carries a 3 fold higher specific activity than *Ps*-XK (Fig. 10). While the activity measured at different temperatures (Fig. 11) or pH (Fig. 12), *Ps*-XK has maximal activity at 37℃ and pH 7 while *Ps*-XKA55T is at 42℃ and pH 7.5. We reason that *Ps*-XKA55T with a single residue change of *Ps*-XK increased tolerance to higher temperature which is a required property for practical use in fermentation process (Dmytruk et al., 2008).

Kinetic parameters of Ps-XK and Ps-XKA55T

The kinetic constants of *Ps*-XK and *Ps*-XKA55T were determined and compared. The kinetics was determined under various concentrations of xylulose or varying the concentration of ATP (Fig.13). After the data fitted to Lineweave-Burk equation, the k_{cat} / K_M revealed the catalytic efficiency of *Ps*-XKA55T for xylulose and ATP were much higher than that of the wild type at 42°C (Table 6).

As shown in Fig. 14, the structure of *Ps*-XKA55T using *Ec*-XK as template was predicted.

Discussion

To construct a *S. cerevisiae* strain which can efficiently grow on D-xylose has been an intense research object. Most of the research has focused on overexpression of the genes involved in the metabolism of xylose (Wahlbom et al., 2003). However, an impaired growth of the engineered strain has been a problem for mass production. Physiological studies have shown that XK is essential for growth on xylose or xylulose and is a limiting factor for the overall rate of pentose sugar utilization. The enzyme has been studied from several prokaryotes and lower eukaryotes to higher eukaryotes.

Rodriguez-Pena *et al*. first suggested the XK overexpression is toxic for *S. cerevisiae* cells grown on D-xylulose (Rodriguez-Pena JM, 1998). The *Sc*-XK as well as *Ps*-XK accepted D-ribulose as a substrate and hence the increased levels of the XK activity should be designed in concert with the capacity of the surrounding metabolic network (Yong-Su Jin, 2003, Richard et al., 2000). Here, we intend to obtain large amounts of a highly efficient and specific XK protein which could be added to the fermenting yeast at a certain stage without impairing the cell growth.

However, the first attempt to engineer the recombinant *Sc*-XK has been failed. No activity could be detected for the heterologously expressed *Sc*-XK and *Sc*-XK (S88V). The previous study demonstrates significant post-transcriptional control of protein levels for a number of different compartments and functional modules. The availability of genome-wide data of mRNA levels, translational status, and protein abundances in yeast was performed an integrated analysis of post-transcriptional

expression regulation in a whole cell. Greenbaum and coworkers discussed three potential reasons for the lack of a perfect correlation between mRNA and protein levels: (i) translational regulation, (ii) difference of *in vivo* protein half-lives, and (iii) the significant amount of experimental error including differences with respect to the experimental conditions. Accordingly, we speculated that post-transcriptional modification, which lacking in the *E. coli* strain, is essential for the activity of the recombinant proteins (Beyer et al., 2004).

The phospho group transfer of sugar kinase has been reported to be promoted by the two highly conserved aspartate residues. As predicted, the Asp17 of *Ps*-XK is essential for the enzymatic activity since the recombinant *Ps*-XKD17A had no activity detected. It has been reported that *Ps*-XK compared to *Sc*-XK is more specific for D-xylulose (Richard et al., 2000). It is likely that the recombinant *Sc*-XK preferred other 5C sugars as substrate.

The *Ps*-XK (A55T) which carries a residue change displayed higher activity than the wild-type XK. The kinetic properties analyzed demonstrated that the substitution of Ala55 increased the XK affinity toward xylulose and ATP. Interestingly, this change also increased apparently the XK activity at high temperature. The analysis of ribbon diagram XK structure as shown in Fig. 14 revealed that the change of side-chain from $–CH_3$ (Ala) to –OH (Thr) closed to the substrate binding site may lead to an increase activity of *Ps*-XK.

Circular dichroism (CD) is often used to assess the degree to which solution pH, buffers, and additives such as sugars, amino acids or salts

alter the thermal stability of target proteins. In addition, protein secondary structure can be determined by CD spectrum within 'far-UV' of 190–250 nm (Ranjbar and Gill, 2009). It is hence, the study of thermal stability of the recombinant XK could be assessed by monitoring the CD spectrum changes with increasing temperatures. Alternatively, a single wavelength can be chosen which monitors specific feature of the protein structure, and the signal at that wavelength recorded continuously as the temperature increased.

The XK protein which exhibits an increased activity under the conditions when the temperature switched from 37°C to 42°C can be very useful while applied in the xylulose utilization process. This thermostable property could also be used in developing superior yeast strains possessing integrated expression systems for the commercial production of ethanol from lignocelluloses.

References

Amore R, W.M., Hollenberg CP (1989). The fermentation of xylose—an analysis of the expression of Bacillus and Actinoplanes xylose isomerase genes in yeast. *Appl Microbiol Biotechnol 30:351–357*.

Bertilsson, M., Andersson, J. & Liden, G. (2008). Modeling simultaneous glucose and xylose uptake in Saccharomyces cerevisiae from kinetics and gene expression of sugar transporters. *Bioprocess Biosyst Eng*, Vol. 31, No. 4**,** pp. 369-77.

Beyer, A., Hollunder, J., Nasheuer, H.P. & Wilhelm, T. (2004). Post-transcriptional expression regulation in the yeast Saccharomyces cerevisiae on a genomic scale. *Mol Cell Proteomics,* Vol. 3, No. 11**,** pp. 1083-92.

Bolen PL, R.K., Freer SN (1986). Affinity purifications of aldose reductase and xylitol dehydrogenase from the xylose-fermenting yeast Pachysolen tannophilus. *Appl Environ Microbiol 52:660–664*.

Bruinenberg PM, d.B.P., van Dijken JP, Scheffers WA (1983). The role of redox balances in the anaerobic fermentation of xylose by yeasts. *Eur J Appl Microbiol Biotechnol 18:287–292*.

Bruinenberg PM, d.B.P., van Dijken JP, Scheffers WA (1984). NADH-linked aldose reductase: the key to anaerobic fermentation of xylose by yeasts. *Appl Microbiol Biotechnol 19:256–260*.

Chan, C.H., Liang, H.K., Hsiao, N.W., Ko, M.T., Lyu, P.C. & Hwang, J.K. (2004). Relationship between local structural entropy and protein thermostability. *Proteins,* Vol. 57, No. 4**,** pp. 684-91.

Chandrakant P, B.V. (1998). Simultaneous bioconversion of cellulose and hemicellulose to ethanol. *Crit Rev Biotechnol 18:295–331*.

Chu, B.C. & Lee, H. (2007). Genetic improvement of Saccharomyces cerevisiae for xylose fermentation. *Biotechnol Adv,* Vol. 25, No. 5**,** pp. 425-41.

Debus D, M.H., Shulze D, Dellweg H (1983). Fermentation of xylose with the yeast Pachysolen tannophilus. *Eur J Appl Microbiol Biotechnol 17:287–291*.

Deng XX, H.N. (1990). Xylulokinase activity in various yeasts including Saccharomyces cerevisiae containing the cloned xylulokinase gene. *Appl Biochem Biotechnol 24–25:193–199*.

Di Luccio, E., Petschacher, B., Voegtli, J., Chou, H.T., Stahlberg, H.,

Nidetzky, B. & Wilson, D.K. (2007). Structural and kinetic studies of induced fit in xylulose kinase from Escherichia coli. *J Mol Biol,* Vol. 365, No. 3**,** pp. 783-98.

Dien, B.S., Cotta, M.A. & Jeffries, T.W. (2003). Bacteria engineered for fuel ethanol production: current status. *Appl Microbiol Biotechnol,* Vol. 63, No. 3**,** pp. 258-66.

Dmytruk, O.V., Dmytruk, K.V., Abbas, C.A., Voronovsky, A.Y. & Sibirny, A.A. (2008). Engineering of xylose reductase and overexpression of xylitol dehydrogenase and xylulokinase improves xylose alcoholic fermentation in the thermotolerant yeast Hansenula polymorpha. *Microb Cell Fact,* Vol. 7**,** pp. 21.

Doelle MB, M.R., Doelle HW (1989). Production of ethanol from corn using inoculum cascading of Zymomonas mobilis. *Process Biochem 24:137–140*.

Eliasson, A., Boles, E., Johansson, B., Osterberg, M., Thevelein, J.M., Spencer-Martins, I., Juhnke, H. & Hahn-Hagerdal, B. (2000). Xylulose fermentation by mutant and wild-type strains of Zygosaccharomyces and Saccharomyces cerevisiae. *Appl Microbiol Biotechnol,* Vol. 53, No. 4**,** pp. 376-82.

Eliasson A, H.J.-H., Pedler S, Hahn-Hägerdal B (2001). The xylose reductase/xylitol dehydrogenase/xylulokinase ratio affects product formation in recombinant xylose-utilising Saccharomyces cerevisiae. *Enzyme Microb Technol 29:288–297*.

Gárdonyi M, H.-H.B. (2003). The Streptomyces rubiginosus xylose isomerase is misfolded when expressed in Saccharomyces cerevisiae. *Enzyme Microb Technol 32:252–259*.

Graves, T., Narendranath, N.V., Dawson, K. & Power, R. (2007). Interaction effects of lactic acid and acetic acid at different temperatures on ethanol production by Saccharomyces cerevisiae in corn mash. *Appl Microbiol Biotechnol,* Vol. 73, No. 5**,** pp. 1190-6.

Ho, N.W., Chen, Z. & Brainard, A.P. (1998). Genetically engineered Saccharomyces yeast capable of effective cofermentation of glucose and xylose. *Appl Environ Microbiol,* Vol. 64, No. 5**,** pp. 1852-9.

Hu, B., Wang, K., Wu, L., Yu, S.H., Antonietti, M. & Titirici, M.M. (2010). Engineering carbon materials from the hydrothermal carbonization process of biomass. *Adv Mater,* Vol. 22, No. 7**,** pp.

813-28.
Ingram, L.O., Conway, T., Clark, D.P., Sewell, G.W. & Preston, J.F. (1987). Genetic engineering of ethanol production in Escherichia coli. *Appl Environ Microbiol*, Vol. 53, No. 10**,** pp. 2420-5.
Jeffries, T.W. (2006). Engineering yeasts for xylose metabolism. *Curr Opin Biotechnol*, Vol. 17, No. 3**,** pp. 320-6.
Jeppsson, M., Traff, K., Johansson, B., Hahn-Hagerdal, B. & Gorwa-Grauslund, M.F. (2003). Effect of enhanced xylose reductase activity on xylose consumption and product distribution in xylose-fermenting recombinant Saccharomyces cerevisiae. *FEMS Yeast Res*, Vol. 3, No. 2**,** pp. 167-75.
Jin, Y.S., Jones, S., Shi, N.Q. & Jeffries, T.W. (2002). Molecular cloning of XYL3 (D-xylulokinase) from Pichia stipitis and characterization of its physiological function. *Appl Environ Microbiol*, Vol. 68, No. 3**,** pp. 1232-9.
Jin YS, J.T. (2003). Changing flux of xylose metabolites by altering expression of xylose reductase and xylitol dehydrogenase in recombinant Saccharomyces cerevisiae. *Appl Biochem Biotechnol 105–108:277–286*.
Johansson, B., Christensson, C., Hobley, T. & Hahn-Hagerdal, B. (2001). Xylulokinase overexpression in two strains of Saccharomyces cerevisiae also expressing xylose reductase and xylitol dehydrogenase and its effect on fermentation of xylose and lignocellulosic hydrolysate. *Appl Environ Microbiol*, Vol. 67, No. 9**,** pp. 4249-55.
Kötter P, C.M. (1993). Xylose fermentation by Saccharomyces cerevisiae. *Appl Microbiol Biotechnol 38:776–783*.
Karhumaa, K., Fromanger, R., Hahn-Hagerdal, B. & Gorwa-Grauslund, M.F. (2007). High activity of xylose reductase and xylitol dehydrogenase improves xylose fermentation by recombinant Saccharomyces cerevisiae. *Appl Microbiol Biotechnol*, Vol. 73, No. 5**,** pp. 1039-46.
Katahira, S., Fujita, Y., Mizuike, A., Fukuda, H. & Kondo, A. (2004). Construction of a xylan-fermenting yeast strain through codisplay of xylanolytic enzymes on the surface of xylose-utilizing Saccharomyces cerevisiae cells. *Appl Environ Microbiol*, Vol. 70, No. 9**,** pp. 5407-14.
Katahira S, I.M., Takema H, Fujita Y, Tanino T, Tanaka T, Fukuda H,

Kondo A (2008). Improvement of ethanol productivity during xylose and glucose co-fermentation by xylose assimilating S. cerevisiae via expression of glucose transporter Sut1. *Enzyme Microb Technol 2008, 43:115-119.*

Kuyper M, H.H., Stave AK, Winkler AA, Jetten MSM, deLaat WTAM, den Ridder JJJ, Op den Camp HJM, van Dijken JP,Pronk JT (2003). High-level functional expression of a fungal xylose isomerase: the key to efficient ethanolic fermentation of xylose by Saccharomyces cerevisiae? *FEMS Yeast Res 4:69–78*.

Kuyper M, H.M., Toirkens MJ, Almering MJH, Winkler AA, van Dijken JP, Pronk JT (2005a). Metabolic engineering of a xylose-isomerase-expressing Saccharomyces cerevisiae strain for rapid anaerobic xylose fermentation. *FEMS Yeast Res 5:399–409*.

Kuyper M, W.A., van Dijken JP, Pronk JT (2004). Minimal metabolic engineering of Saccharomyces cerevisiae for efficient anaerobic xylose fermentation: a proof of principle. *FEMS Yeast Res 4:655–664*.

Lee, H.J., Chang, H.Y., Venkatesan, N. & Peng, H.L. (2008). Identification of amino acid residues important for the phosphomannose isomerase activity of PslB in Pseudomonas aeruginosa PAO1. *FEBS Lett,* Vol. 582, No. 23-24**,** pp. 3479-83.

Lee, T.H., Kim, M.D., Park, Y.C., Bae, S.M., Ryu, Y.W. & Seo, J.H. (2003). Effects of xylulokinase activity on ethanol production from D-xylulose by recombinant Saccharomyces cerevisiae. *J Appl Microbiol,* Vol. 95, No. 4**,** pp. 847-52.

Lynd, L.R., Cushman, J.H., Nichols, R.J. & Wyman, C.E. (1991). Fuel Ethanol from Cellulosic Biomass. *Science,* Vol. 251, No. 4999**,** pp. 1318-1323.

Madhavan A, T.S., Ushida K, Kanai D, Katahira S, Srivastava A, Fukuda H, Bisaria VS, Kondo A (2008). Xylose isomerase from polycentric fungus Orpinomyces: gene sequencing, cloning and expression in Saccharomyces cerevisiae for bioconversion of xylose to ethanol. *Appl Microbiol Biotechnol doi:10.1007/s00253-008-1794-6*.

Matsushika, A., Inoue, H., Kodaki, T. & Sawayama, S. (2009a). Ethanol production from xylose in engineered Saccharomyces cerevisiae strains: current state and perspectives. *Appl Microbiol Biotechnol,* Vol. 84, No. 1**,** pp. 37-53.

Matsushika, A., Inoue, H., Murakami, K., Takimura, O. & Sawayama, S.

(2009b). Bioethanol production performance of five recombinant strains of laboratory and industrial xylose-fermenting Saccharomyces cerevisiae. *Bioresour Technol,* Vol. 100, No. 8**,** pp. 2392-8.

Matsushika, A., Inoue, H., Watanabe, S., Kodaki, T., Makino, K. & Sawayama, S. (2009c). Efficient bioethanol production by a recombinant flocculent Saccharomyces cerevisiae strain with a genome-integrated NADP+-dependent xylitol dehydrogenase gene. *Appl Environ Microbiol,* Vol. 75, No. 11**,** pp. 3818-22.

Matsushika, A. & Sawayama, S. (2008). Efficient bioethanol production from xylose by recombinant saccharomyces cerevisiae requires high activity of xylose reductase and moderate xylulokinase activity. *J Biosci Bioeng,* Vol. 106, No. 3**,** pp. 306-9.

Millichip RJ, D.H. (1989). Large-scale ethanol production from Milo (Sorghum) using Zymomonas mobilis. *Process Biochem 24:141–145*.

Moes CJ, P.I., van Zyl WH (1996). Cloning and expression of the Clostridium thermosulfurogenes D-xylose isomerase gene (xylA) in Saccharomyces cerevisiae. *Biotechnol Lett 18:269–274*.

Ni, H., Laplaza, J.M. & Jeffries, T.W. (2007). Transposon mutagenesis to improve the growth of recombinant Saccharomyces cerevisiae on D-xylose. *Appl Environ Microbiol,* Vol. 73, No. 7**,** pp. 2061-6.

Ranjbar, B. & Gill, P. (2009). Circular dichroism techniques: biomolecular and nanostructural analyses- a review. *Chem Biol Drug Des,* Vol. 74, No. 2**,** pp. 101-20.

Richard, P., Toivari, M.H. & Penttila, M. (2000). The role of xylulokinase in Saccharomyces cerevisiae xylulose catabolism. *FEMS Microbiol Lett,* Vol. 190, No. 1**,** pp. 39-43.

Rizzi M, E.P., Bui-Thanh NA, Dellweg H (1988). Xylose fermentation by yeasts. 4. Purification and kinetic studies of xylose reductase from Pichia stipitis. *Appl Microbiol Biotechnol 29:148–154*.

Rizzi M, H.K., Erlemann P, Bui-Thanh NA, Dellweg H (1989). Purification and properties of the NAD+-xylitol-dehydrogenase from the yeast Pichia stipitis. *J Ferment Bioeng 67:20–24*.

Rodriguez-Pena, J.M., Cid, V.J., Arroyo, J. & Nombela, C. (1998). The YGR194c (XKS1) gene encodes the xylulokinase from the budding yeast Saccharomyces cerevisiae. *FEMS Microbiol Lett,* Vol. 162, No. 1**,** pp. 155-60.

Rodriguez-Pena JM, C.V., Arroyo J, Nombela C (1998). The YGR194c (XKS1) gene encodes the xylulokinase from the budding yeast Saccharomyces cerevisiae. *FEMS Microbiol Lett 162:155–160*.

Sarthy, A.V., McConaughy, B.L., Lobo, Z., Sundstrom, J.A., Furlong, C.E. & Hall, B.D. (1987). Expression of the Escherichia coli xylose isomerase gene in Saccharomyces cerevisiae. *Appl Environ Microbiol,* Vol. 53, No. 9**,** pp. 1996-2000.

Shamanna, D.K. & Sanderson, K.E. (1979). Uptake and catabolism of D-xylose in Salmonella typhimurium LT2. *J Bacteriol,* Vol. 139, No. 1**,** pp. 64-70.

Skotnicki, M.L., Lee, K.J., Tribe, D.E. & Rogers, P.L. (1982). Genetic alteration of Zymomonas mobilis for ethanol production. *Basic Life Sci,* Vol. 19**,** pp. 271-90.

Tantirungkij M, N.N., Seki T, Yoshida T (1993). Construction of xylose-assimilating Saccharomyces cerevisiae. *J Ferment Bioeng 75:83–88*.

Toivari, M.H., Ruohonen, L., Miasnikov, A.N., Richard, P. & Penttila, M. (2007). Metabolic engineering of Saccharomyces cerevisiae for conversion of D-glucose to xylitol and other five-carbon sugars and sugar alcohols. *Appl Environ Microbiol,* Vol. 73, No. 17**,** pp. 5471-6.

Van Vleet, J.H. & Jeffries, T.W. (2009). Yeast metabolic engineering for hemicellulosic ethanol production. *Curr Opin Biotechnol,* Vol. 20, No. 3**,** pp. 300-6.

Verduyn, C., Van Kleef, R., Frank, J., Schreuder, H., Van Dijken, J.P. & Scheffers, W.A. (1985). Properties of the NAD(P)H-dependent xylose reductase from the xylose-fermenting yeast Pichia stipitis. *Biochem J,* Vol. 226, No. 3**,** pp. 669-77.

Wahlbom, C.F., van Zyl, W.H., Jonsson, L.J., Hahn-Hagerdal, B. & Otero, R.R. (2003). Generation of the improved recombinant xylose-utilizing Saccharomyces cerevisiae TMB 3400 by random mutagenesis and physiological comparison with Pichia stipitis CBS 6054. *FEMS Yeast Res,* Vol. 3, No. 3**,** pp. 319-26.

Walfridsson M, A.M., Bao X, Hahn-Hägerdal B (1997). Expression of different levels of enzymes from the Pichia stipitis XYL1 and XYL2 genes in Saccharomyces cerevisiae and its effects on product formation during xylose utilisation. *Appl Microbiol Biotechnol 48:218–224*.

Walfridsson M, B.X., Anderlund M, Lilius G, Bülow L, Hahn-Hägerdal B (1996). Ethanolic fermentation of xylose with Saccharomyces cerevisiae harboring the Thermus thermophilus xylA gene, which expresses an active xylose (glucose) isomerase. *Appl Environ Microbiol 62:4648–4651*.

Wang, P.Y., and H. Schneider (1980). Growth of yeasts on D-xylulose. *Can. J. Microbiol. 26:1165–1168.*

Wang VW, J.T. (1990). Purification and properties of xylitol dehydrogenase from the xylose-fermenting Candida shehatae. *Appl Biochem Biotechnol 26:197–206*.

Yong-Su Jin, H.N., Jose M. Laplaza, Thomas W. Jeffries (2003). Optimal Growth and Ethanol Production from Xylose by Recombinant Saccharomyces cerevisiae Require Moderate D-Xylulokinase Activity. *APPLIED AND ENVIRONMENTAL MICROBIOLOGY, Jan. 2003, p. 495–503*.

Table 1 Bacterial and yeast used in this study

Strain	Genotype or relevant characteristic	source
E. coli:		
BL21-RIL	*F⁻ ompT hsdSB(rB⁻mB⁻)gal dcm*(DE3)	Laboratory stock
JM109	*RecA1 supE44 endA1 hsdR17 gyrA96 rolA1 thi* △*(lac-proAB)*	Laboratory stock
NovaBlue(DE3)	*endA1 hsdR17*(rk12⁻ mk12⁺) *supE44 thi-1 recA1gyrA96 relA1 lac*[F' *pro AB lac*^{q}Z △M15:: Tn*10*](DE3); Tet^{R}	Laboratory stock
XL1-blue(DE3)	*recA endA1 gyrA96 thi-1 hsdR17 supE44 relA1 lac*[F' *pro AB lac*^{q}Z△M15:: Tn*10*](DE3); Tet^{R}	Laboratory stock
***Pichia stipitis* CBS 6054**	Wild type	Laboratory stock
***Saccharomyces cerevisiae* S288c**	Wild type	Laboratory stock

Table 2 Plasmids used and constructed in this study

Plasmids	Description	Reference or source
YT&A vector	PCR cloning vector, Ap^R	Yeastern Biotech
pET-30b	Expression vector, Km^R	Novagene
p*Ps*-XK	A 1.8-kb fragment of *XYL1* cloned into Y&T vector, Ap^R	This study
p*Ps*-XKA55T	p*Ps*-XK derivative with a mutation A55T on XK	This study
p*Ps*-XKD17A	p*Ps*-XK derivative with a mutation D17A on XK	This study
pET30-*Ps*-XK	An *Eco*RI/*Sal*I fragment containing the coding sequence of *Ps*-XK cloned into pET30b with XK-His6-tag fusion XK, Km^R	This study
pET30-*Ps*-XKA55T	pET30-*Ps*-XK derivative with a mutation A55T on XK	This study
pET30-*Ps*-XKD17A	pET30-*Ps*-XK derivative with a mutation D17A on XK	This study
p*Sc*-XK	A 1.8-kb fragment of *XKS1* cloned into Y&T vector, Ap^R	This study
p*Sc*-XKS88V	p*Sc*-XK derivative with a mutation S88V on XK	This study

pET30-*Sc*-XK	An *Eco*RI/*Sal*I fragment containing the coding sequence of *Sc*-XK cloned into pET30b with XK-His6-tag fusion XK, Km^R	This study
pET30- *Sc*-XKS88V	pET30-*Sc*-XK derivative with a mutation S88V on XK	This study

Table 3 Primers used in this study

Primer	Sequences (5' to 3')
PJ001	GGCAGGATCACTCTACCGGTAAAG
PJ002	TGCCCATGTAGTGTCAGCATGTG
PJ003	ACGAAAAGCTCTTGGCCATCGCTG
PJ004	TGAACTTGTCCCACGACTTCTTG
PJ017	CTTCCTCGGGTTCGCTCTTTCGACTCAGC
PJ018	GCTGAGTCGAAAGAGCGAACCCGAGGAAG
PJ025	CTAGATCTGGTTCTCGTGAAATATCGCGAG
PJ026	CTCGCGATATTTCACGAGAACCAGATCTAG
PJ035	TTTGGTGACTTGTACACTGATGGAAAGAAG
PJ036	ATGTTGTGTTCAGTAATTCAGAGACAG
PJ037	TTAGATGAGAGTCTTTTCCAGTTCGC
PJ038	ATGACCACTACCCCATTTGATGC
PJ039	TTAGTGTTTCAATTCACTTTCC

Table 4 Condition for XK activity assay

Compound	Working concentration	Stock concentration	Working Vol (µl)
Tris-HCl	50 mM	100 mM	500
$MgCl_2$	5 mM	250 mM	20
NADH	0.2 mM	10 mM	20
PEP	1 mM	50 mM	20
Xylulose	8.5 mM	425 mM	20
ATP	2 mM	100 mM	20
LDH	10 U	0.665 U/µl	15
PK	1.5U	1.0317U/µl	1.5
XK	variable		
H_2O	variable		
Total			1000

Table 5 Entropy analysis of specific amino acids on *Sc*-XK

Position	Amino acid	Entropy	Displace Amino acid	Varied entropy
47	S	1.628351	E	1.167115
88	S	1.682168	V	1.207951
169	G	1.62045	C	1.259718
253	S	1.687964	W	1.320305
254	S	1.807884	M	1.398319
255	S	1.731955	W	1.491264

The entropy change was calculated by replacing the target amino acid with other nineteen amino acids and the minimum entropy state was selected.

Table 6 Kinetics comparison of *Ps*-XK and *Ps*-XKA55T

Strain	**Substrate(mM)**	V_{max}(mMmin^{-1})	K_M(mM)	k_{cat}(min^{-1})	k_{cat}/K_M(min^{-1}mM^{-1})
Ps-XK	xylulose	0.05±0.01	0.39±0.05	3800.68±419.88	9772.52±1092.69
	ATP	0.06±0.01	0.52±0.11	4399.25±627.68	9036.70±3029.22
Ps-XKA55T	xylulose	0.06±0.01	0.31±0.07	4177.78±457.83	14784.55±5096.93
	ATP	0.06±0.004	0.41±0.15	4543.88±305.10	13755.79±7505.71

The values were obtained from the initial velocity data and nonlinear regression analysis of from $V = V\max\ [S]h/\ ([S]h + Kmh)$ as described in Material and Methods.

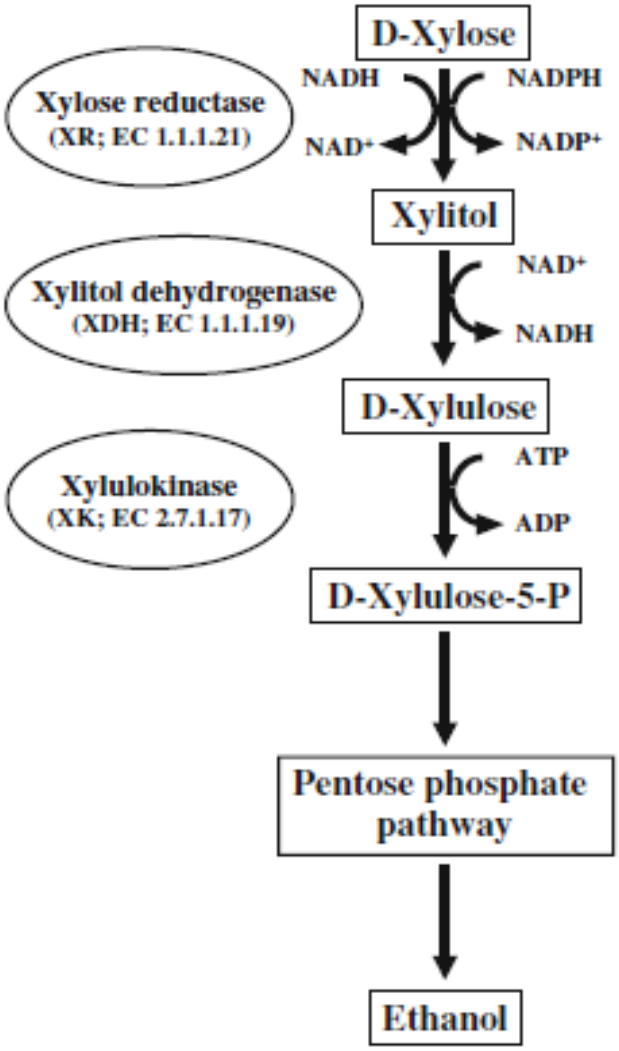

Fig. 1. The fermentation pathway of microbial transformation of D-Xylose to ethanol. The D-xylose is reduced to xylitol by XR; the xylitol is oxidized to xylulose by XDH, and then the xylulose is phosphorylated by xylulokinase (XK) to xylulose 5-phosphate (X5P). The X5P is eventually metabolized through the pentose phosphate pathway (PPP) and glycolysis to ethanol (Yong-Su Jin, 2003).

Pichia stipitis

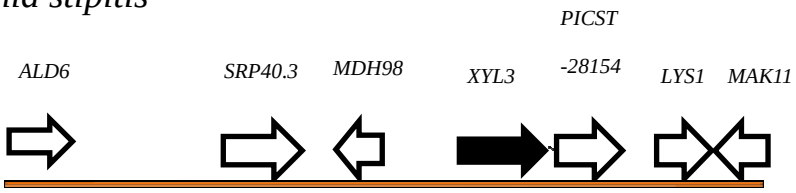

Saccharomyces cerevisiae

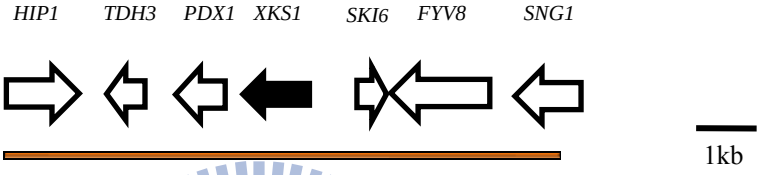

Fig. 2. Comparison of the gene organization of *Ps*-XK and *Sc*-XK. The gene clusters containing XK gene and the flanking loci of *Pichia stipitis* and *Saccharomyces cerevisiae* are shown. The XK encoding genes *XYL3* and *XKS1* are marked solid black.

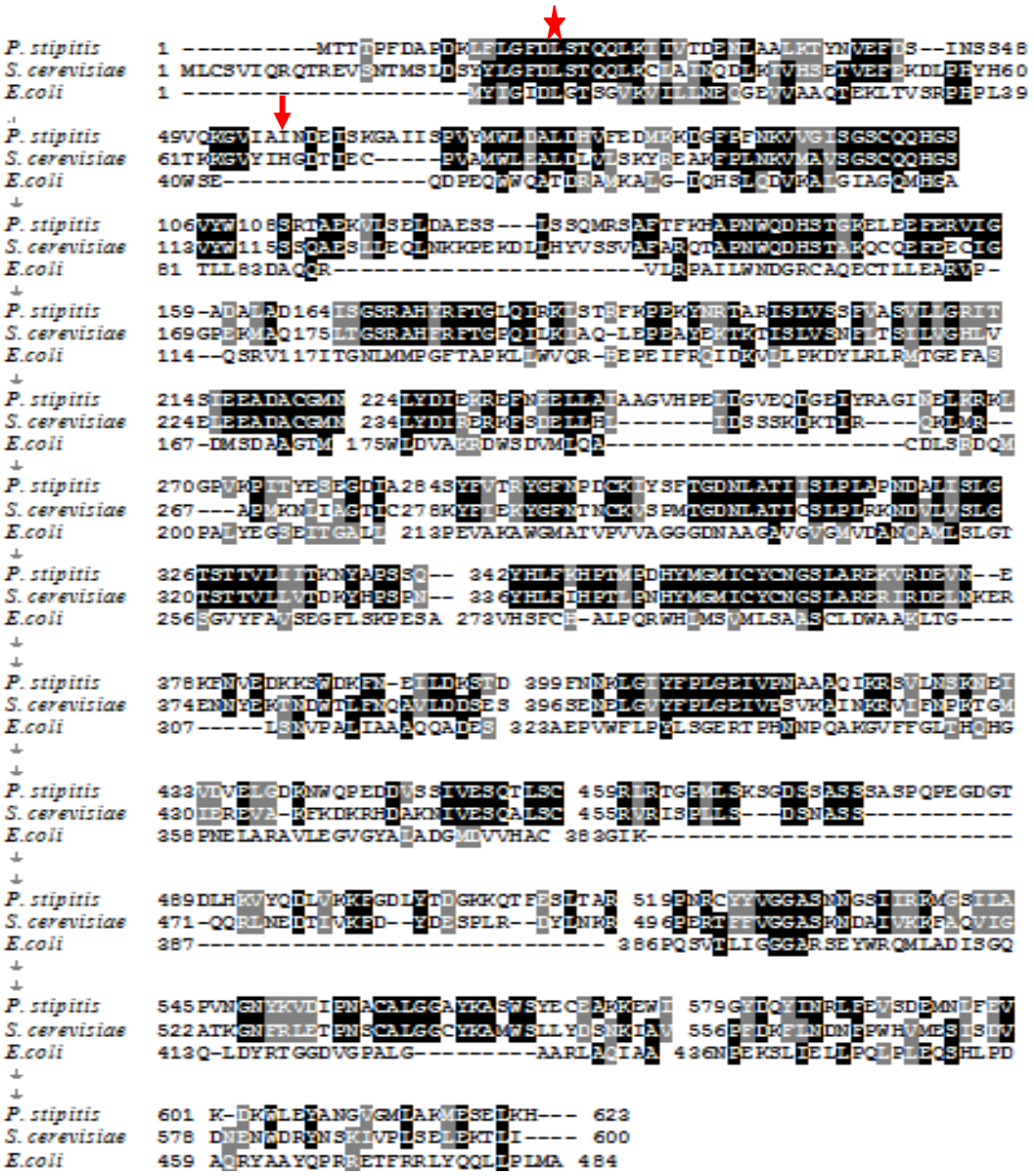

Fig. 3. Amino acid sequence alignment of *Ps*-XK and *Sc*-XK. The N-terminal peptide LGFDLSTQQLK has been shown to be involved in phosphate binding (Jin et al., 2002). The aspartic acid marked by a star sign is essential for XK activity (Di Luccio et al., 2007). The arrow indicates the position of the threonine residue mutated in this study.

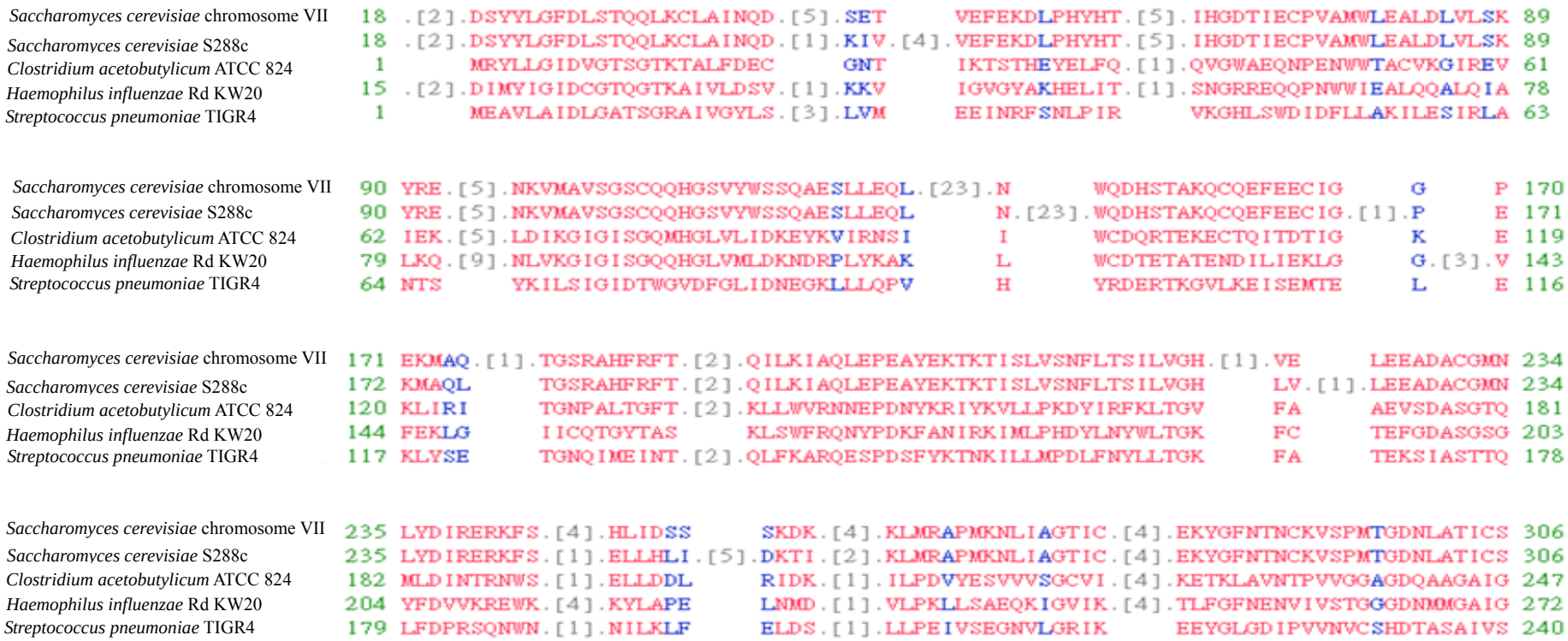

Fig. 4. Selected residues of *Sc*-XK for entropy state analysis. The conserved residues were colored red. The blue residues were selected for the analysis of entropy change (http://blast.ncbi.nlm.nih.gov/Blast.cgi).

(A)

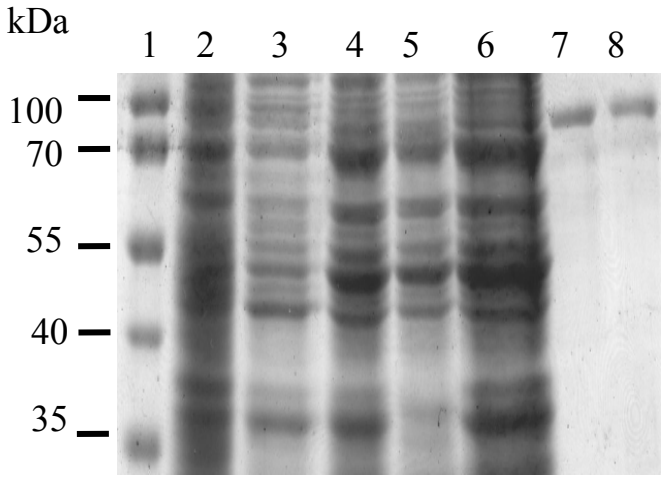

(B)

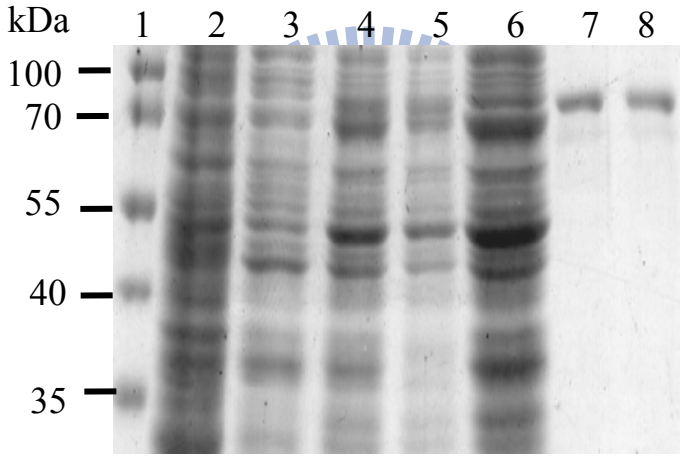

Fig. 5. Expression and purification of the recombinant *Sc*-XK (A) and *Sc*-XKS88V (B). The *XKS1* gene was isolated and cloned into pET30b, and the resulting plasmid transformed into *E. coli* NovaBlue (DE3). Cell lysates of the bacteria grown overnight at 22℃ in 500 ml LB medium with or without addition of 0.5 mM IPTG were isolated and then resolved by SDS-PAGE. Lanes 1, protein markers with molecular weights as indicated; 2 and 3, *E. coli* NovaBlue (DE3) [pET30b] and NovaBlue (DE3) [pET30b-XK] without IPTG induction; 4, NovaBlue (DE3) [pET30b-XK] induced with IPTG; 5, supernatant of the sample 4; 6, pellet of the sample 4; 7 and 8, purified XK (~74-kDa).

(A)

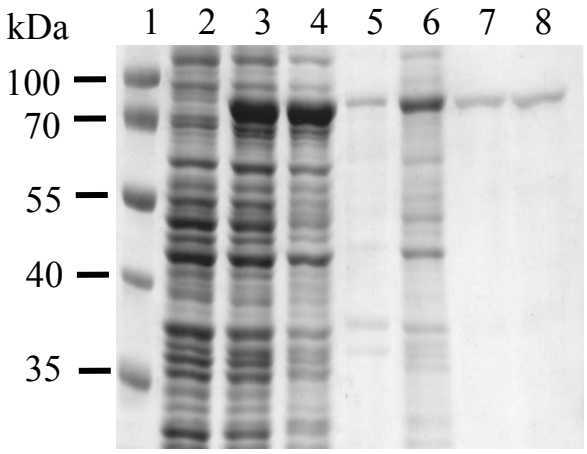
kDa
1 2 3 4 5 6 7 8
100
70
55
40
35

(B)

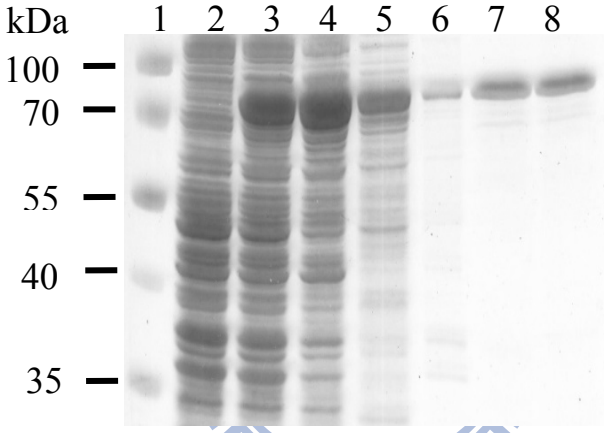
kDa
1 2 3 4 5 6 7 8
100
70
55
40
35

(C)

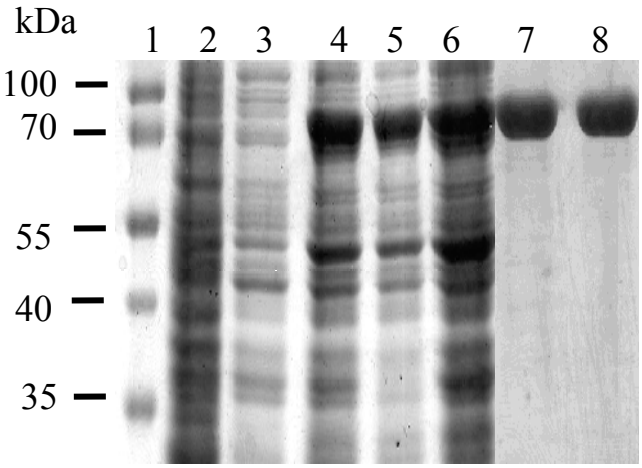
kDa
1 2 3 4 5 6 7 8
100
70
55
40
35

Fig. 6. Overexpression and purification of the recombinant *Ps*-XK (A), *Ps*-XKA55T (B) and *Ps*-XKD17A (C). The *XYL3* gene was isolated and cloned into pET30b, and the resulting plasmid transformed into *E. coli* BL-21(DE3). Cell lysates of the bacteria grown overnight at 22℃ in 500 ml LB medium with or without addition of 0.5mM IPTG were isolated and then resolved by SDS-PAGE. Lanes1, protein markers with molecular weights as indicated; 2 and 3, *E. coli* BL-21(DE3) [pET30b] and BL-21(DE3) [pET30b-XK] without IPTG induction; 4, BL-21(DE3)[pET30b-XK] induced with IPTG; 5, supernatant of the sample 4; 6, pellet of the sample 4; 7 and 8, purified XK (~75-kDa).

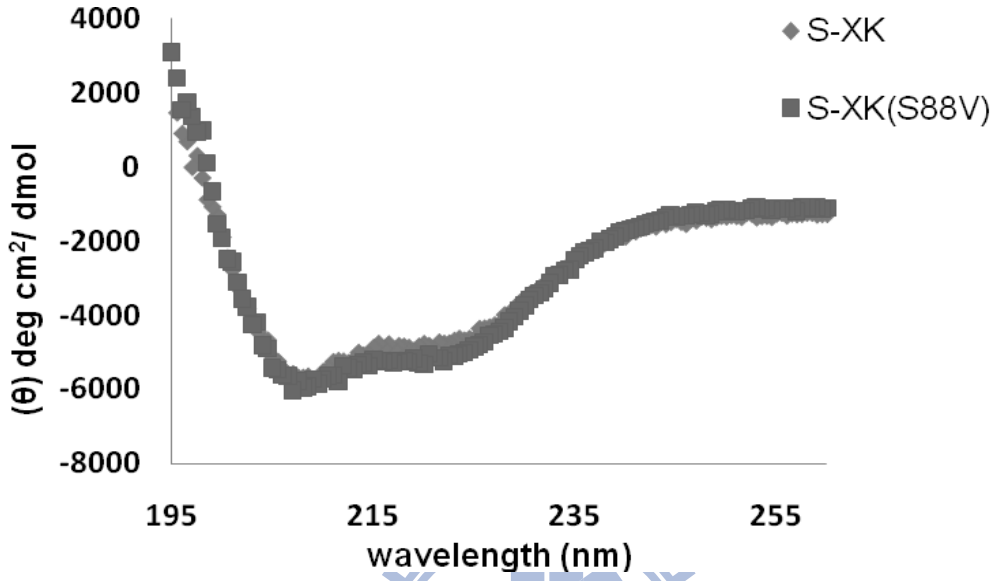

Fig. 7. Circular dichroism spectra of the recombinant *Sc*-XK and *Sc*-XKS88V. The measurement was carried out at 25 ℃ in 10 mM Tris-HCl, pH 7.4.

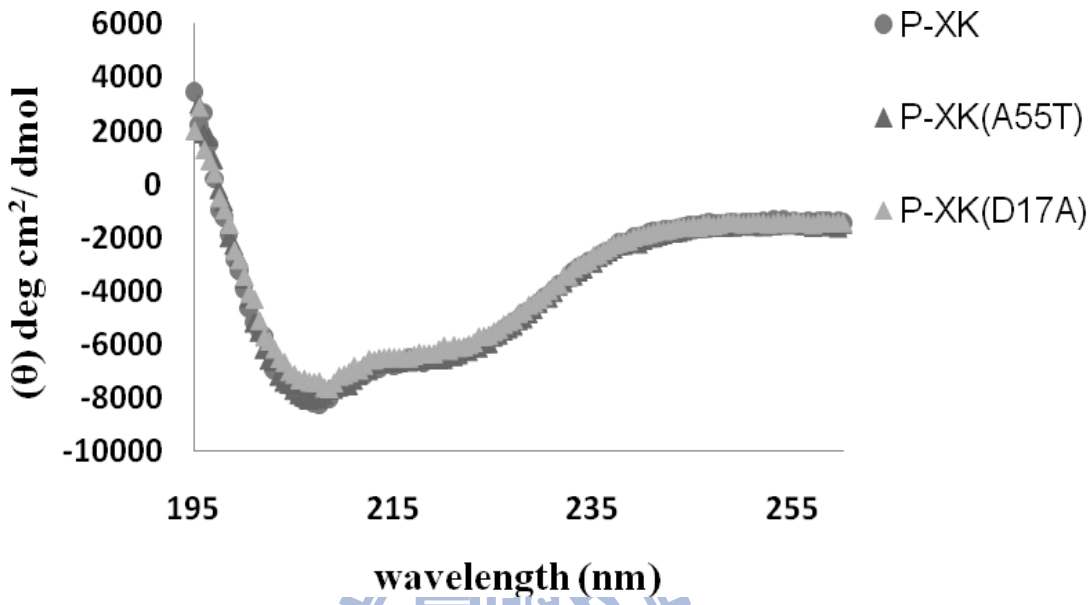

Fig. 8. Circular dichroism spectra of the recombinant *Ps*-XK, *Ps*-XKA55T and *Ps*-XKD17A. The measurement was carried out at 25 ℃ in 10 mM Tris-HCl, pH 7.4.

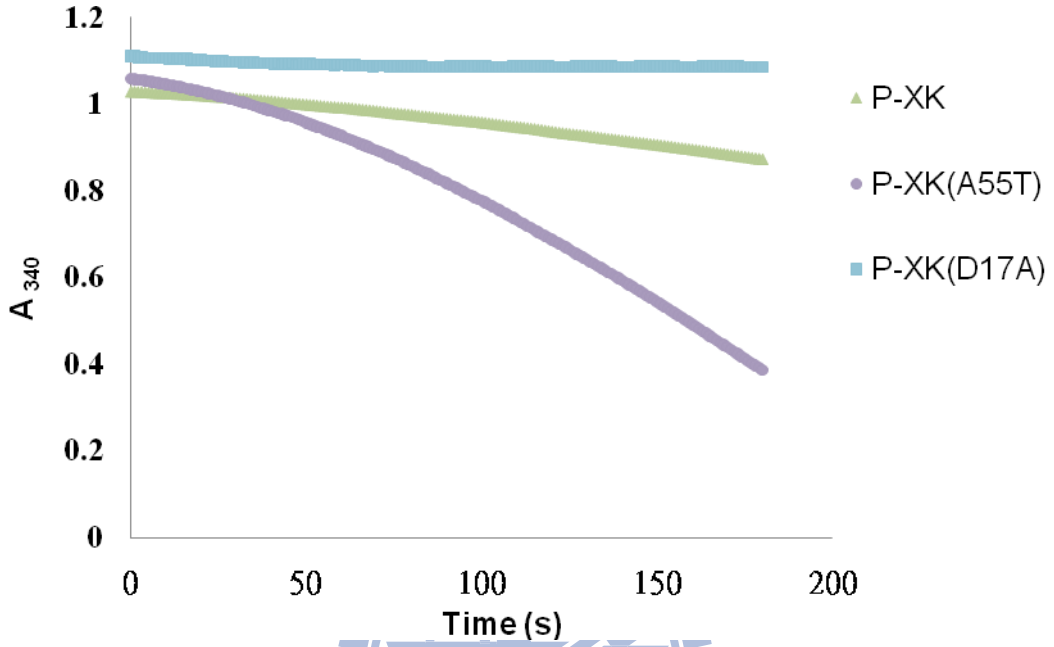

Fig. 9. Enzymatic activity analysis of *Ps*-XK, *Ps*-XKA55T and *Ps*-XKD17A. The activity measurement was carried out for 5 μl *Ps*-XK, 1 μl *Ps*-XKA55T and 0.5 μl *Ps*-XKD17A respectively at 25℃ in 50 mM Tris-HCl, pH 7.8 and the decrease of NADH determined by the absorption at 340 nm.

(A)

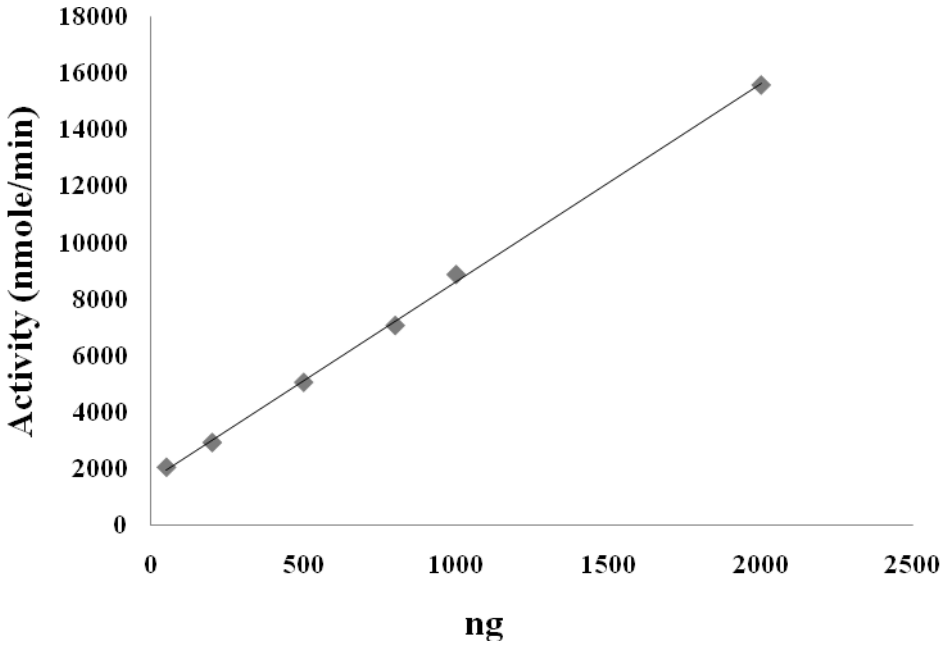

(B)

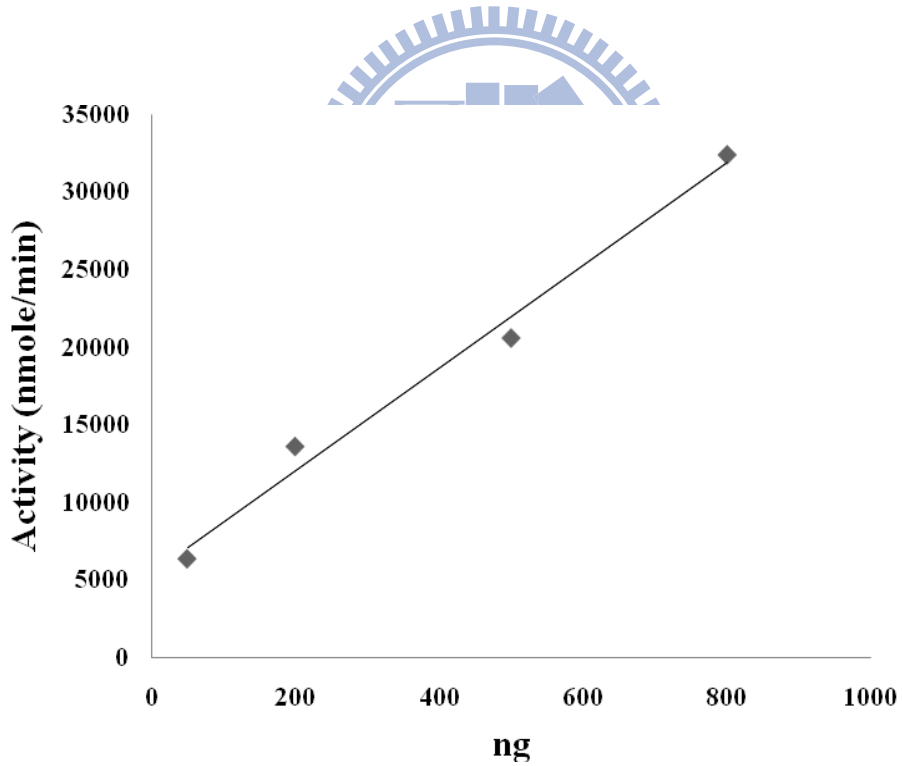

Fig. 10. Measurement of the specific activity for *Ps*-XK (A) and *Ps*-XKA55T (B). The activity measurement was carried out at 25℃ in 50 mM Tris-HCl, pH 7.8 and the decrease of NADH determined by the absorption at 340 nm.

(A)

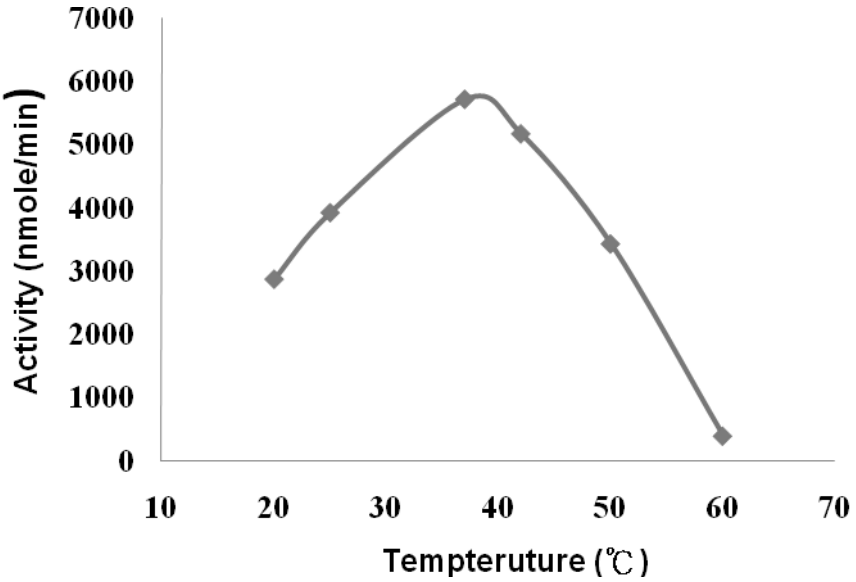

(B)

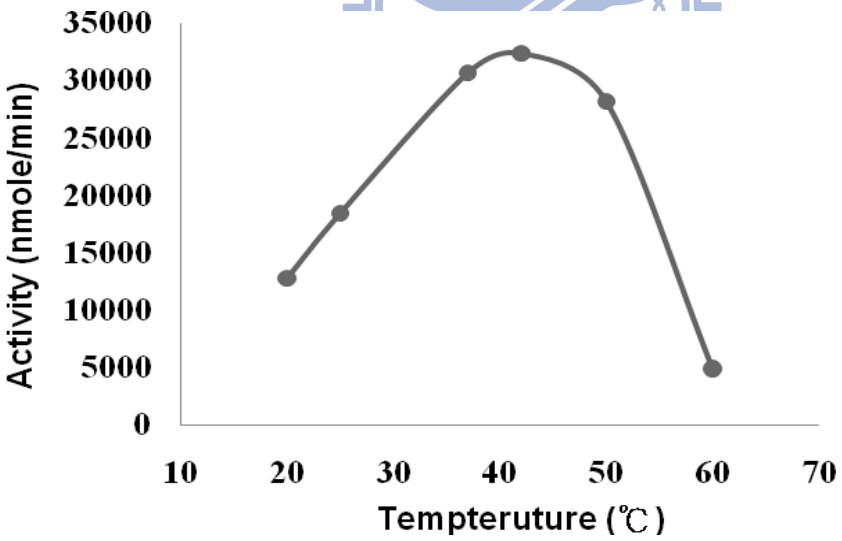

Fig. 11. Temperature effect on the activity of *Ps*-XK (A) and *Ps*-XKA55T (B). The activity measurement was carried out with 0.5μg protein in 50 mM Tris-HCl, pH 7.8 at 20℃, 25℃, 37℃, 42℃, 50℃, and 60℃, respectively.

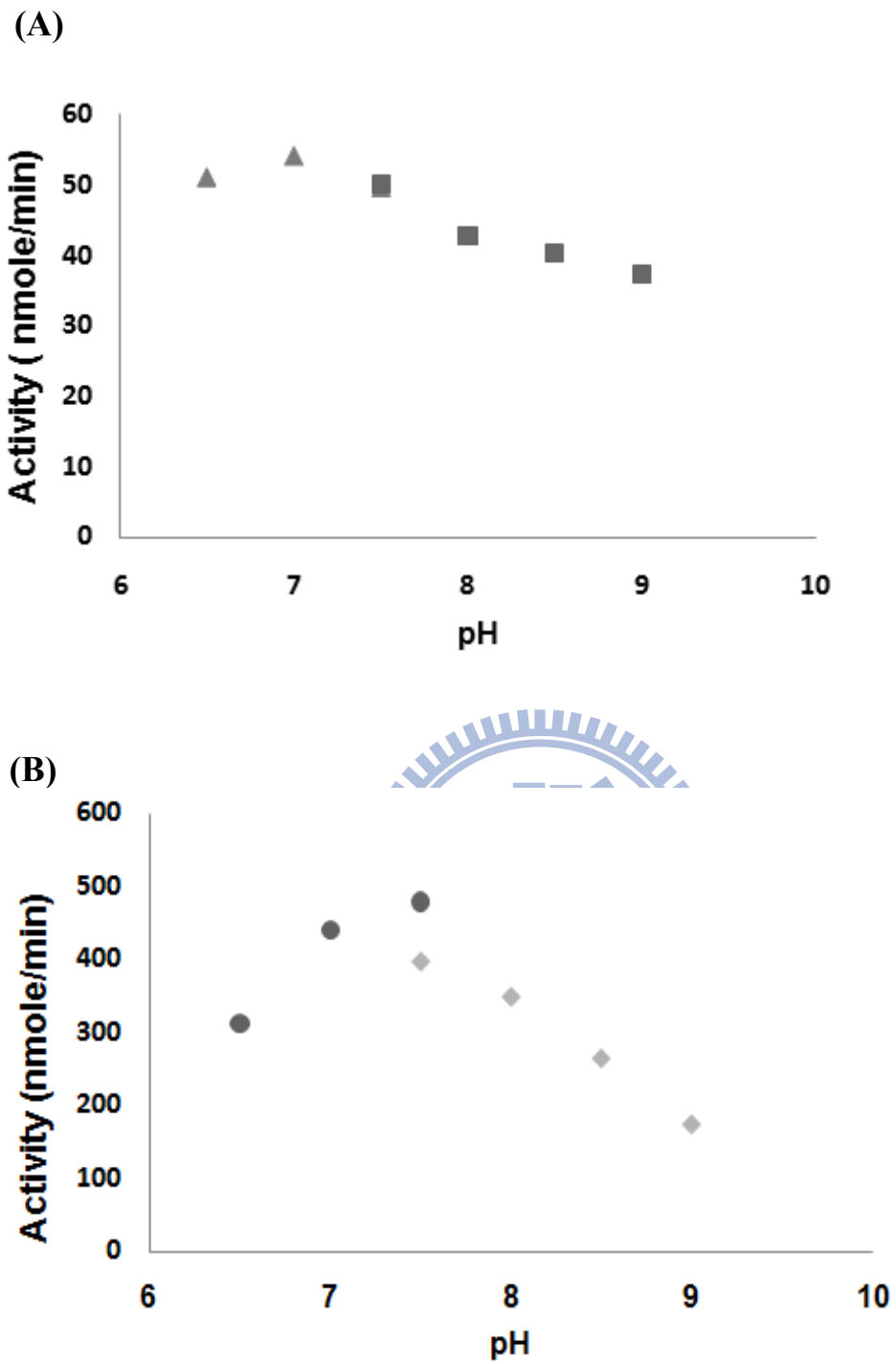

Fig. 12. Effect of the pH change on the activity of *Ps*-XK (A) and *Ps*-XKA55T (B). The activity measurement was carried out with 0.5μg protein at 25℃ in pH 6.5, pH 7 and pH 7.5 Tris-HCl and pH 7.5, pH 8, pH 8.5 and pH 9 MPOS, respectively.

(A)

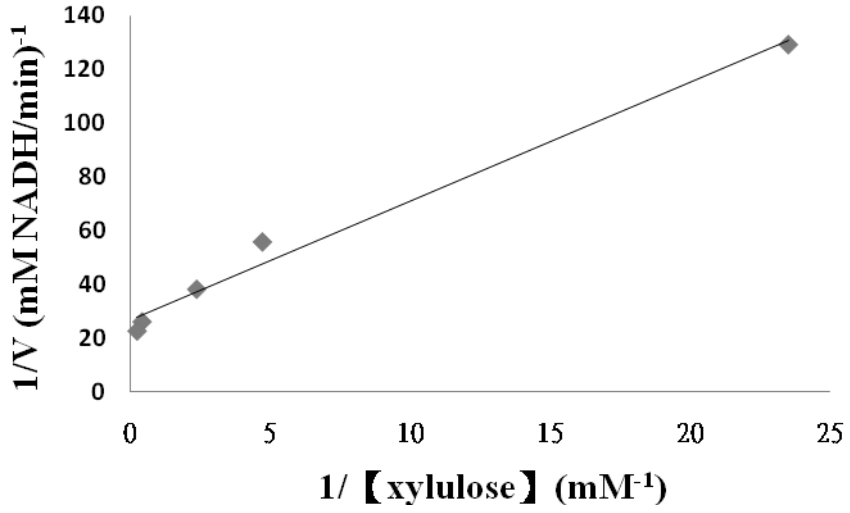
1/V (mM NADH/min)-1
140
120
100
80
60
40
20
0
0
5
10
15
20
25
1/【xylulose】(mM-1)

(B)

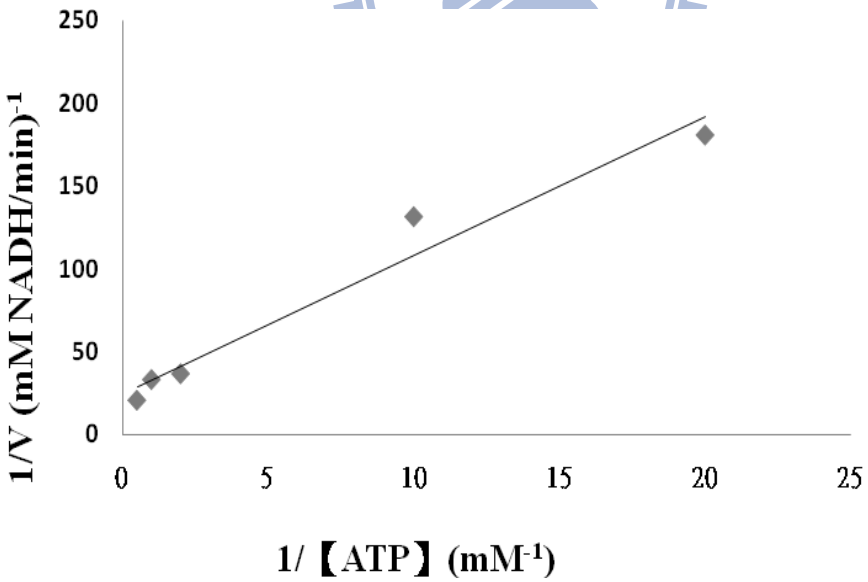
1/V (mM NADH/min)-1
250
200
150
100
50
0
0
5
10
15
20
25
1/【ATP】(mM-1)

(C)

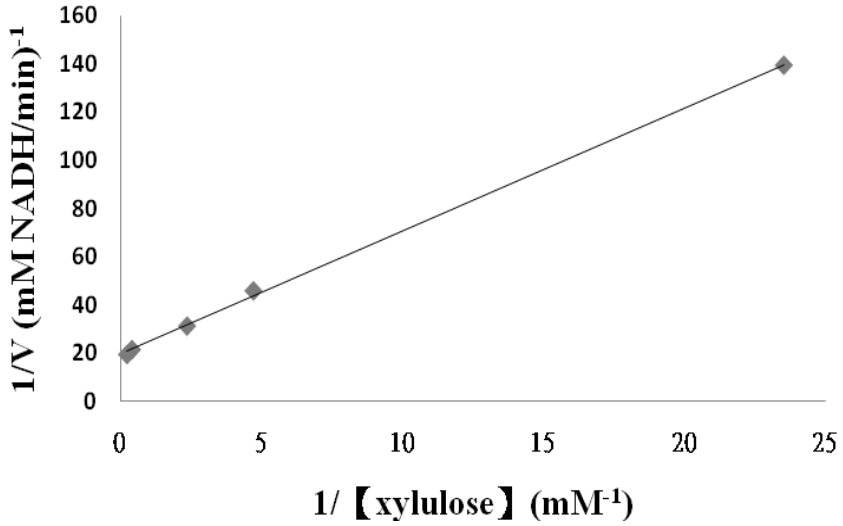

(D)

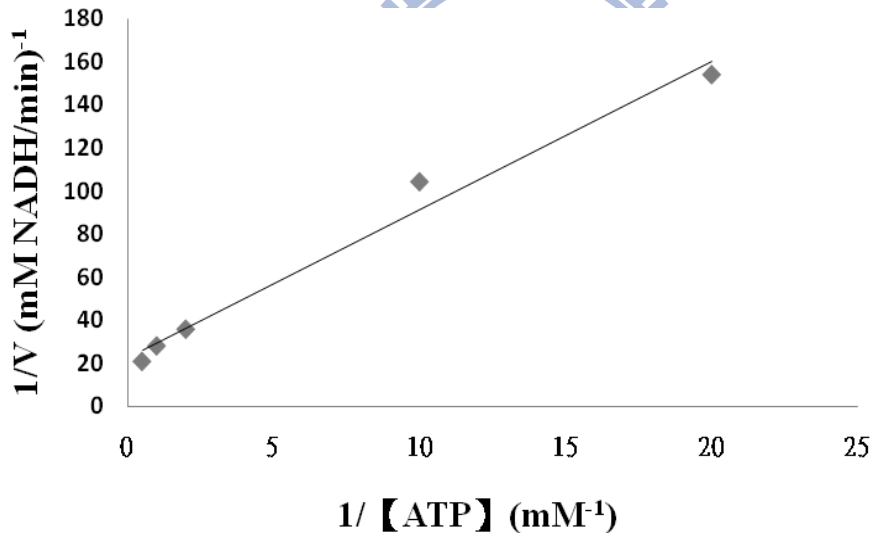

Fig. 13. Kinetics studies of *Ps*-XK and *Ps*-XKA55T. The study uses variable amounts of xylulose or ATP. The substrate of xylulose level with 0.0425 mM, 0.2125 mM, 0.425 mM, 2.5 mM or 4.5 mM and ATP concentration with 0.05 mM, 0.1 mM, 0.5 mM, 1 mM or 2mM were used for each determination. The activity measurement was carried out at 42℃in 50 mM Tris-HCl, pH 7.8 and the decrease of NADH determined by the absorption at 340 nm. (A) Xylulose *Ps*-XK, (B) ATP *Ps*-XK,(C) Xylulose *Ps*-XKA55T, (D) ATP *Ps*-XKA55T.

(A)

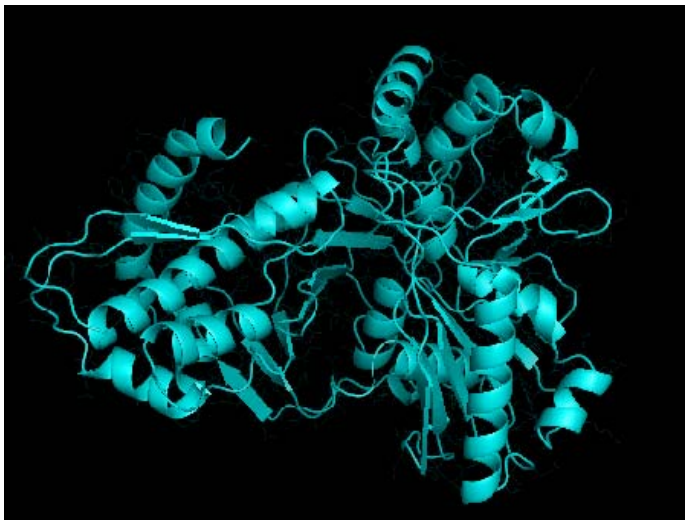

(B)

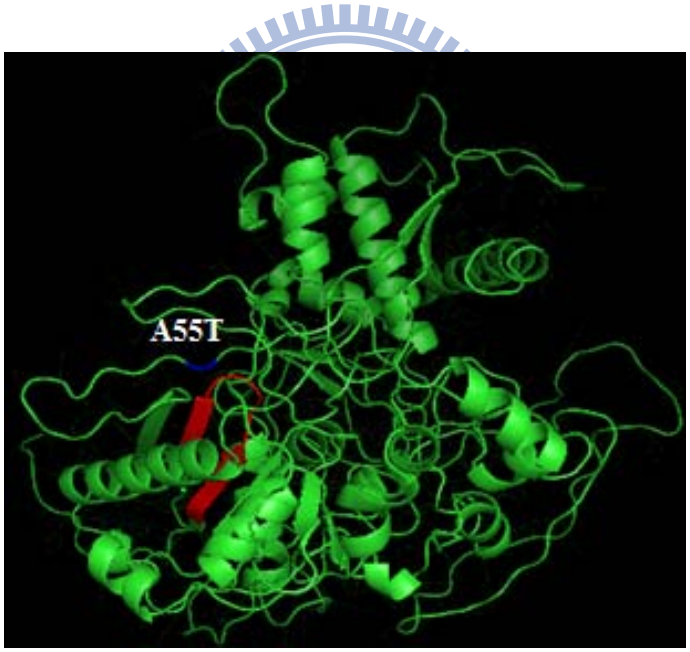

Fig.14. Ribbon diagram of the XK structure (A) Structure of *E.coli* XK (B) The predicted structure for *Ps*-XKA55T. Position of the threonine residue is colored blue and the phosphate binding site (Jin et al., 2002) is colored red.

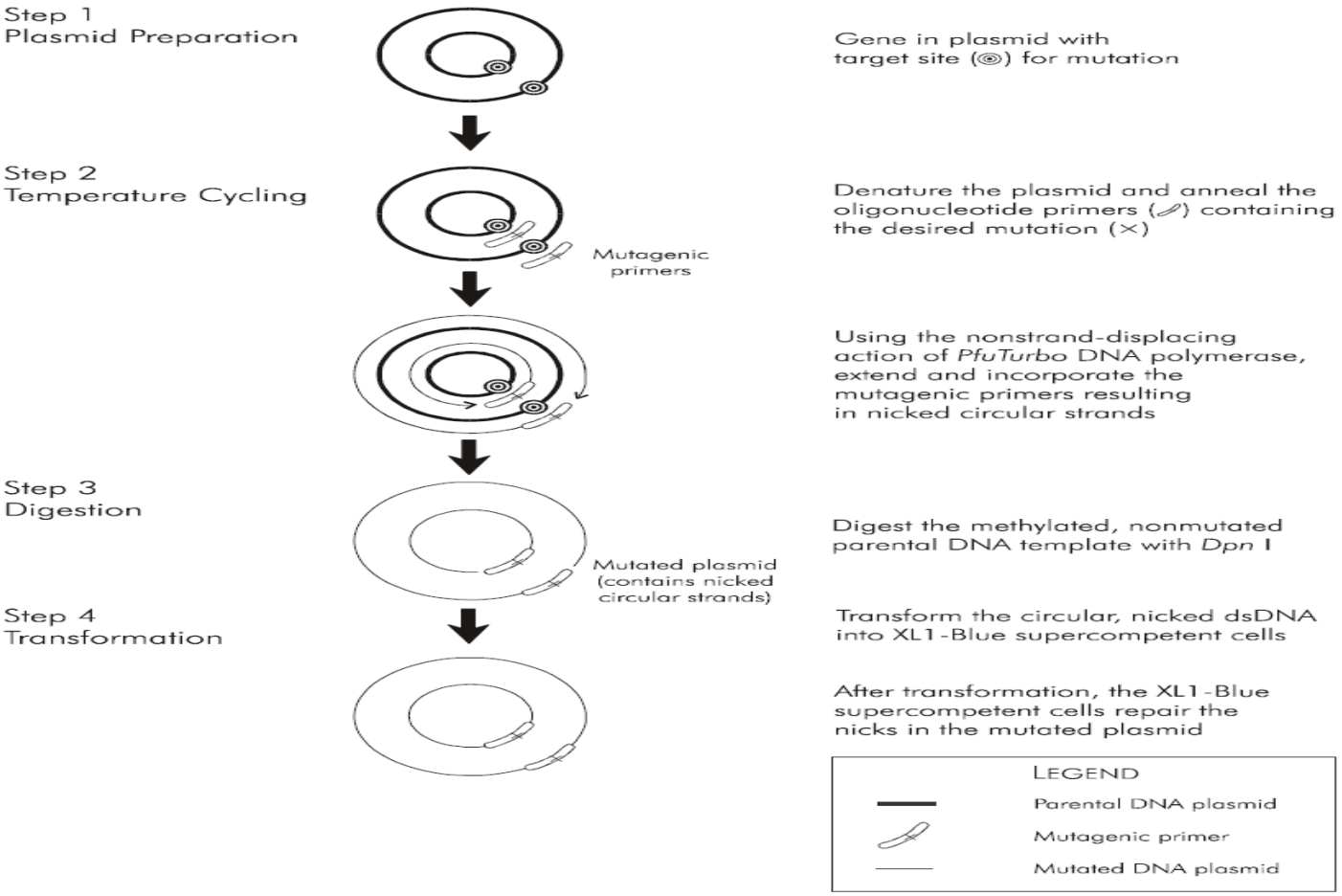

Appendix. 1. Overview of the site-directed mutagenesis method (QuikChange® Site-Directed Mutagenesis Kit INSTRUCTION MANUAL).

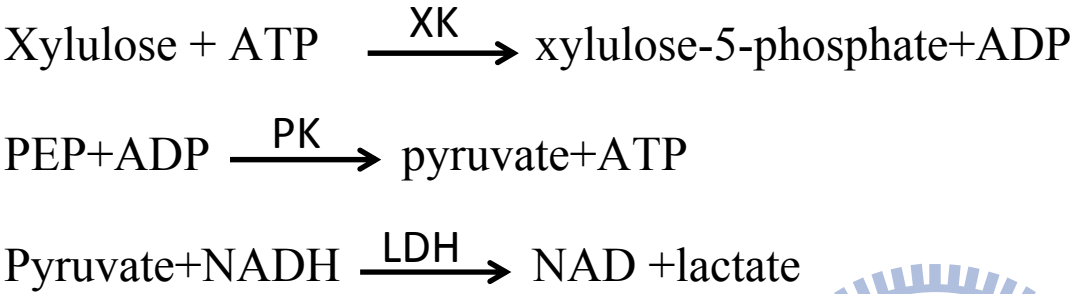

Appendix 2. XK activity assay was carried out according to the coupled reaction. The reaction was started with addition of the purified XK. Xylulose is phosphorylated into xylulose 5-phosphate via XK. PEP is oxidized to pyruvate by ADP-dependent PK and then pyruvate is reduced to lactate by NADH-dependent LDH. The absorption of NADH was measured at 340 nm(Shamanna and Sanderson, 1979).


E
S
A
1896


E
S
A
1896


E S A
1896